WISPs, WIMPs, and Gammas

Searches for Dark Matter and New Physics with Fermi Large Area Telescope

COSMIC WISPERS
CA21106

Milena Crnogorčević (she/her)
Postdoctoral Fellow at the Oskar Klein Centre
milena.crnogorcevic@fysik.su.se

April 24, 2024

Stockholm University

Dark Matter Landscape: A Theorist's View

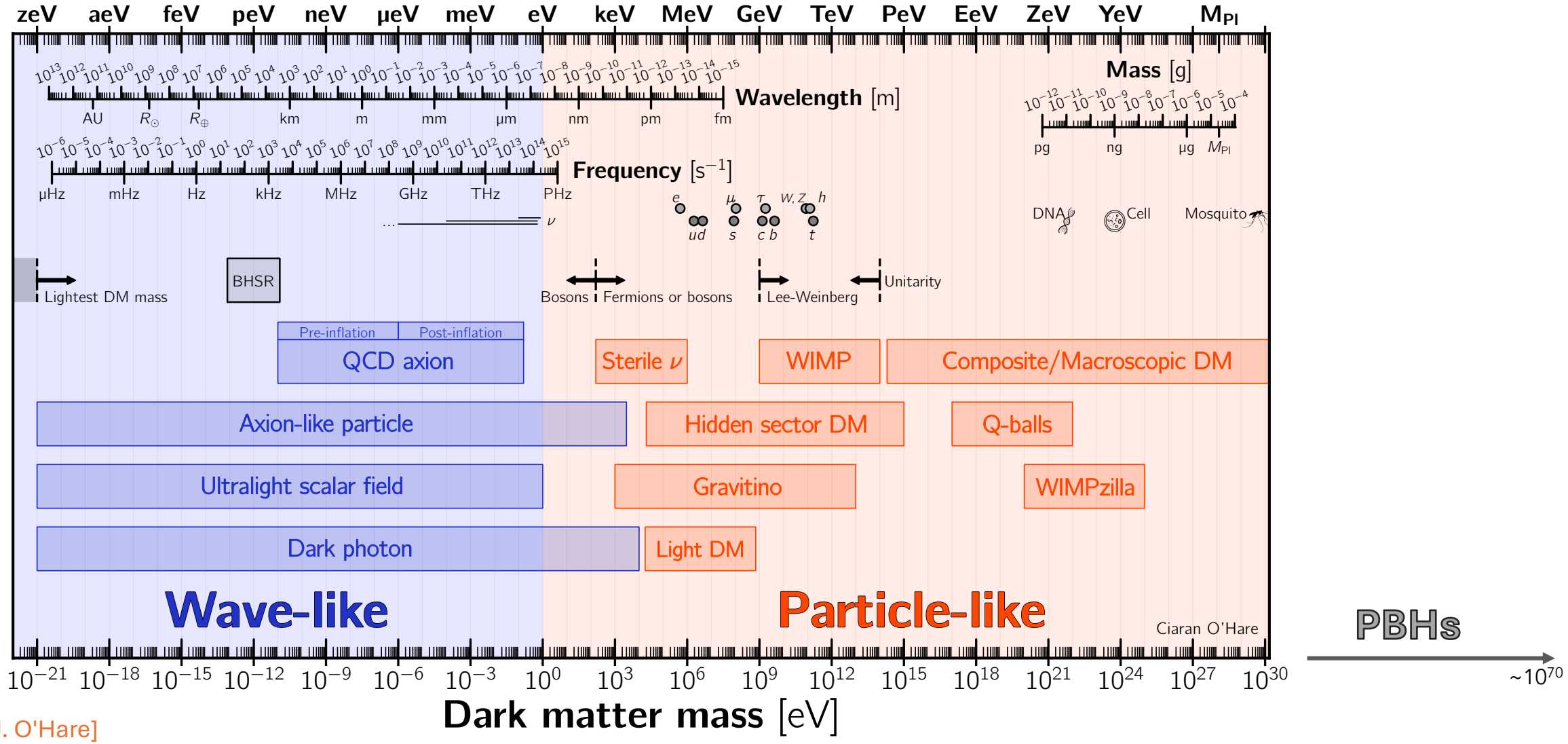

[Ciaran A. J. O'Hare]

Dark Matter Landscape: An Observer's View

Overwhelming *indirect* evidence for the existence of dark matter

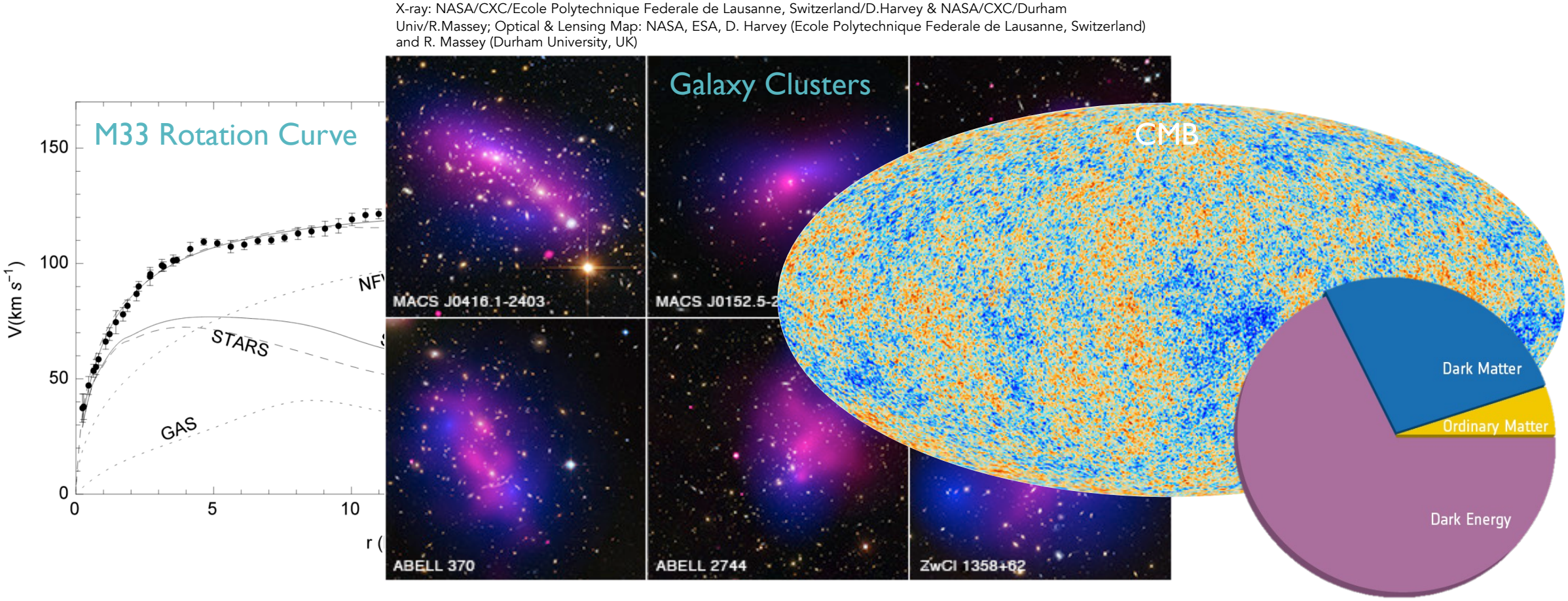

Dark Matter Landscape: An Observer's View

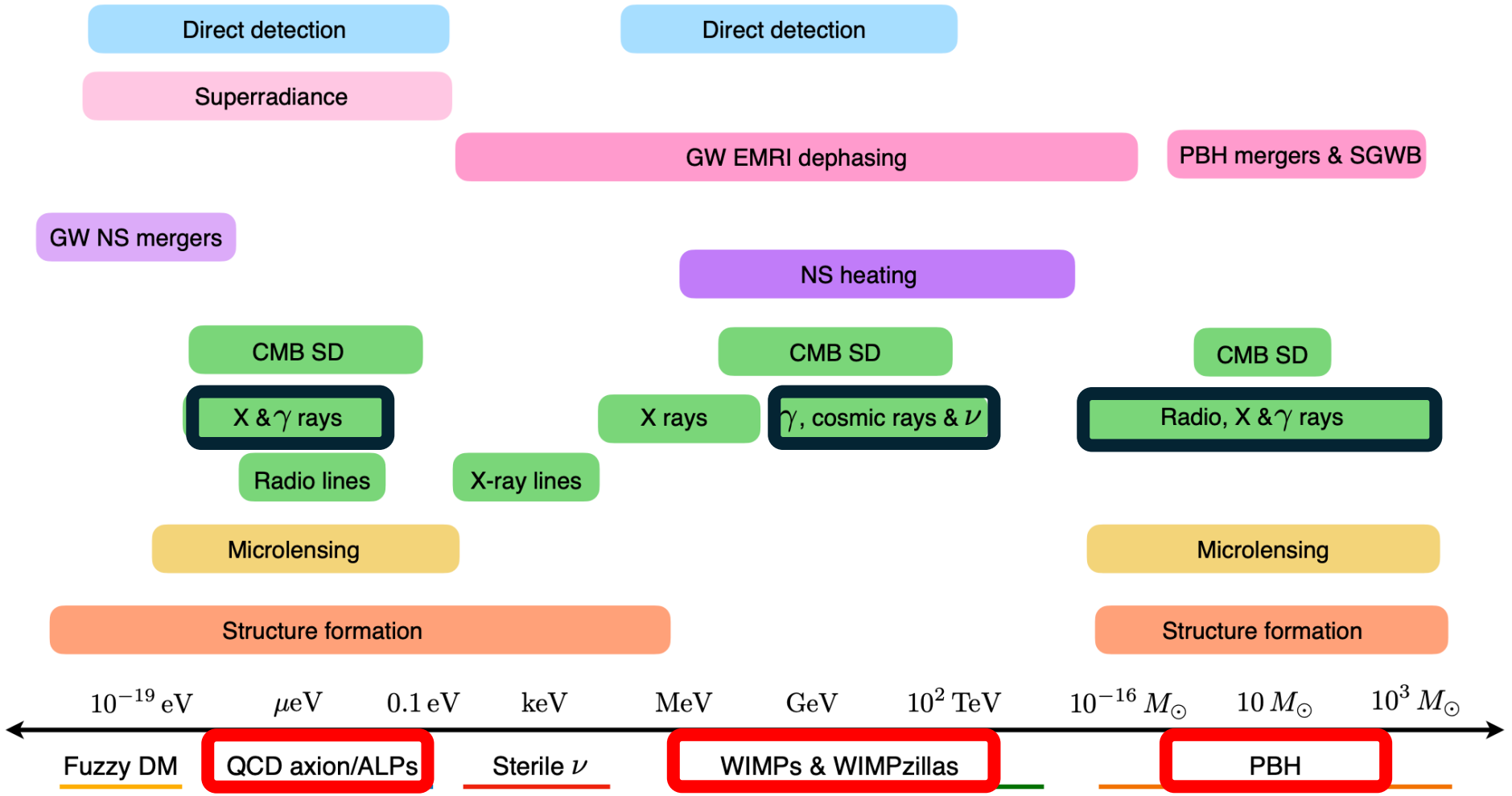

[EuCAPT WhitePaper, 2021]

Observing ALPs with Gamma Rays

In the presence of an external magnetic field, **B**, axion-like particles (ALPs) undergo a conversion into photons:

$$\mathcal{L}_{a\gamma} \supset g_{a\gamma}\, \mathbf{E} \cdot \mathbf{B}\, a$$

where $g_{a\gamma}$ is ALP-photon coupling rate, and a is the ALP field strength.

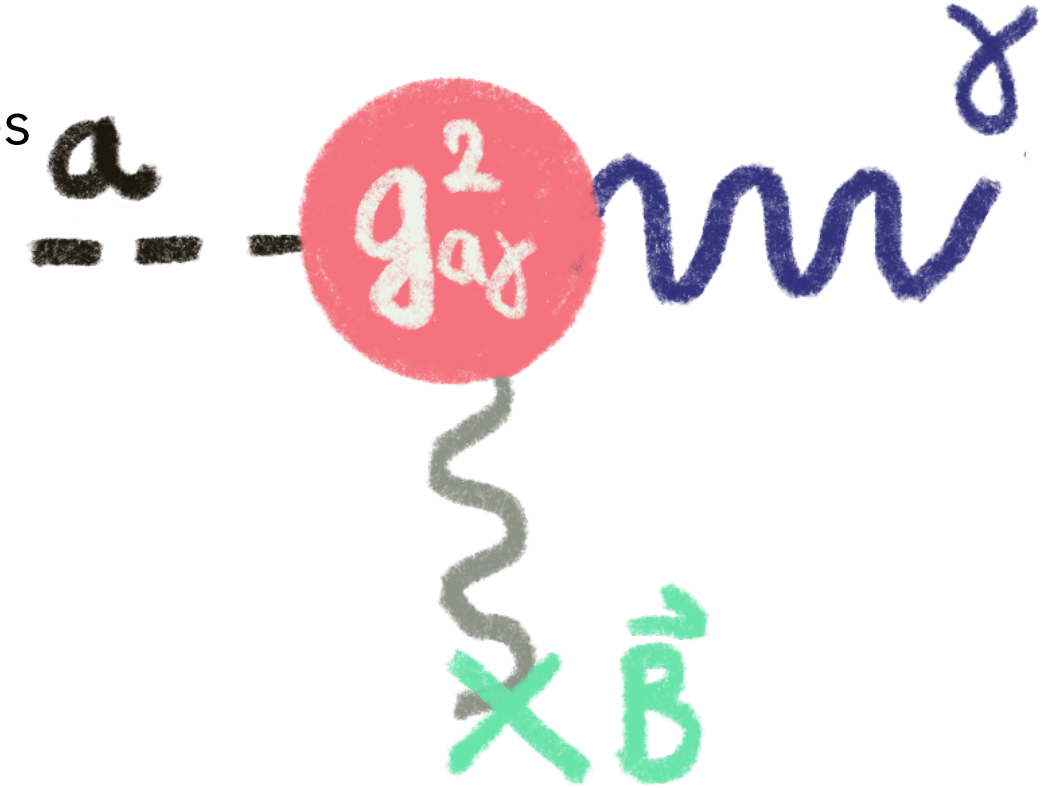

Observing ALPs with Gamma Rays

Primakoff process: converting ALPs into photons

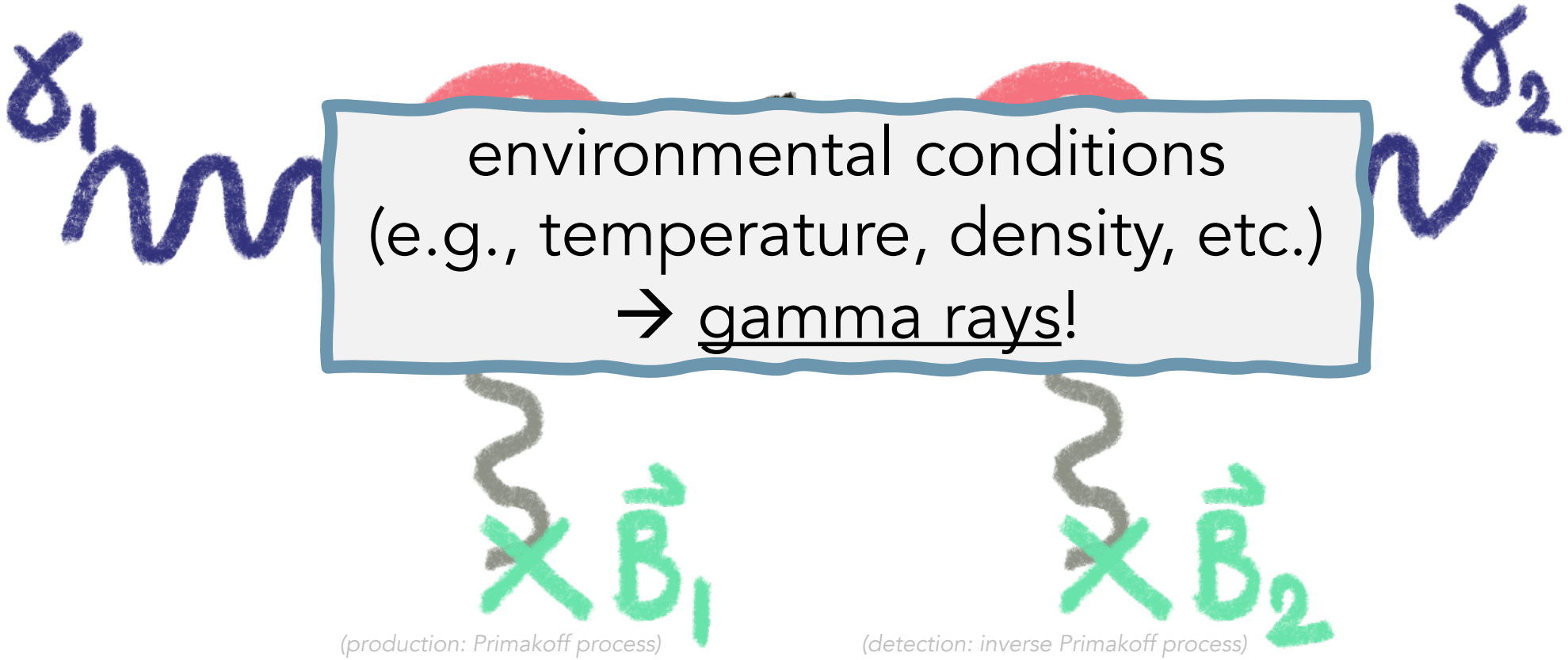

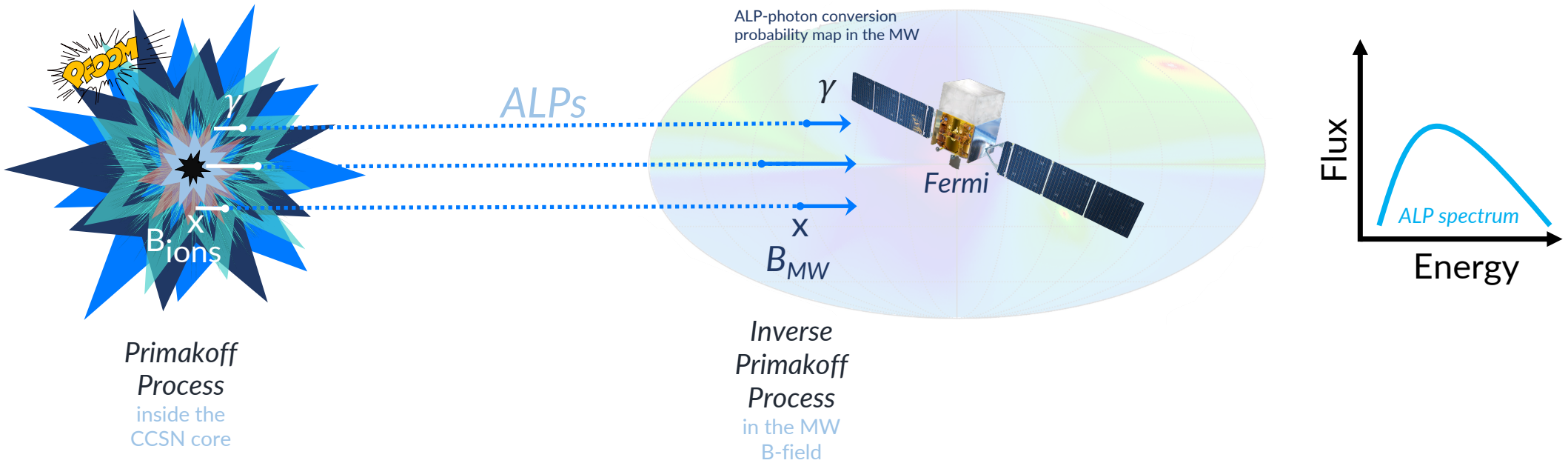

Primakoff Process inside the CCSN core

Inverse Primakoff Process in the MW B-field

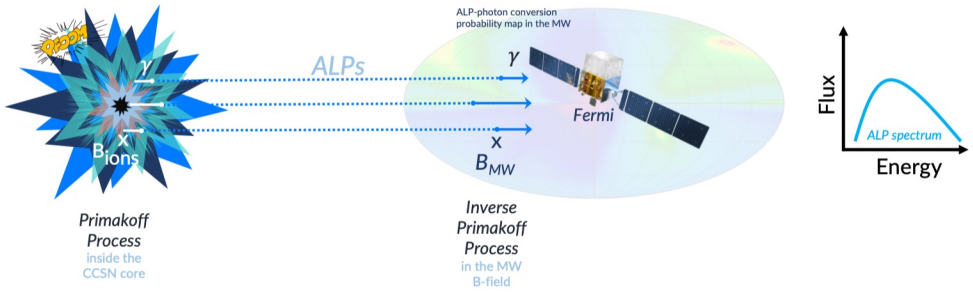
ALPs
γ
X
B ions
Primakoff Process
inside the CCSN core
ALP-photon conversion probability map in the MW
γ
X
B MW
Fermi
Inverse Primakoff Process
in the MW B-field
Flux
ALP spectrum
Energy

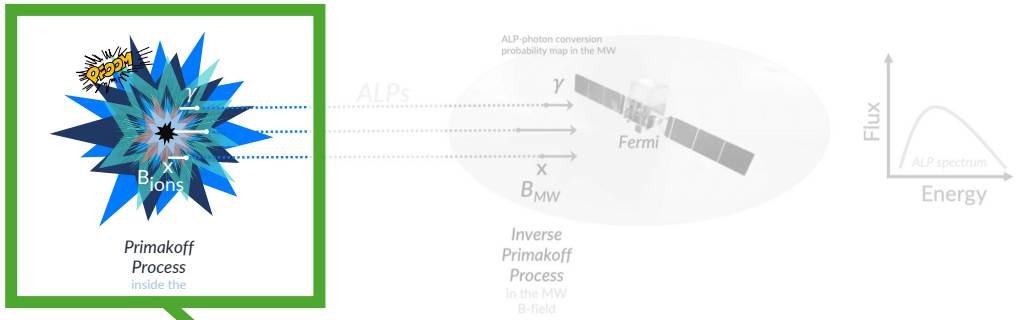

CCSN --- Long Gamma-ray Burst relationship

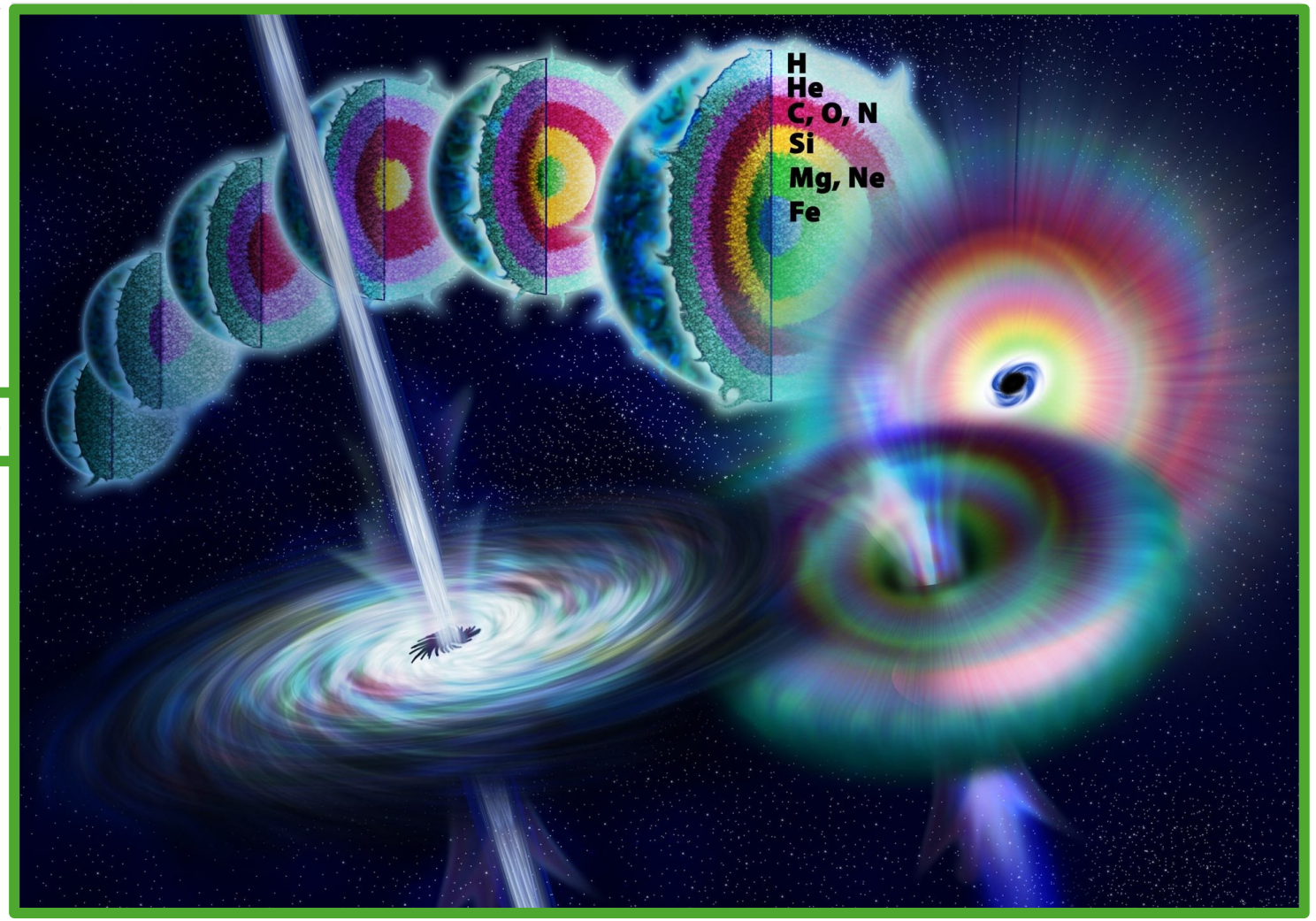

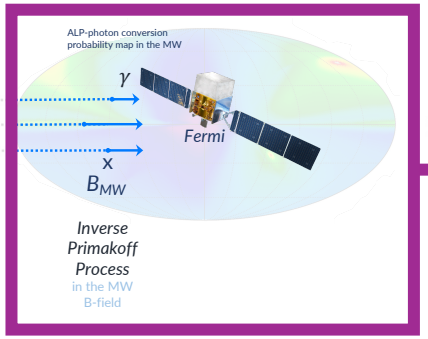

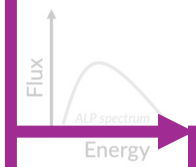

Assumptions: magnetic fields: only considering the MW magnetic field, neglecting IGMF

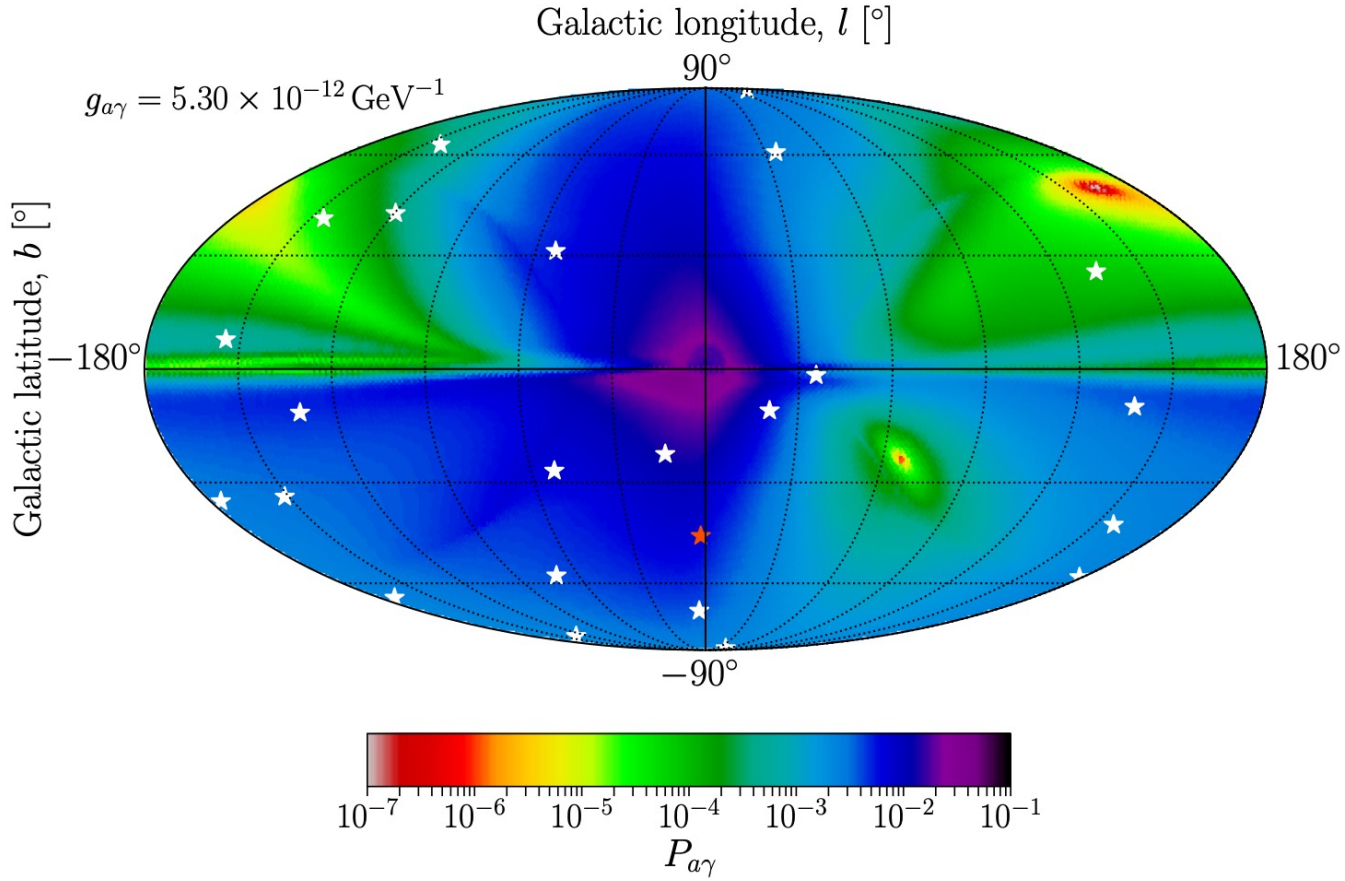

ALP-photon conversion probability map in the Milky Way's magnetic field.

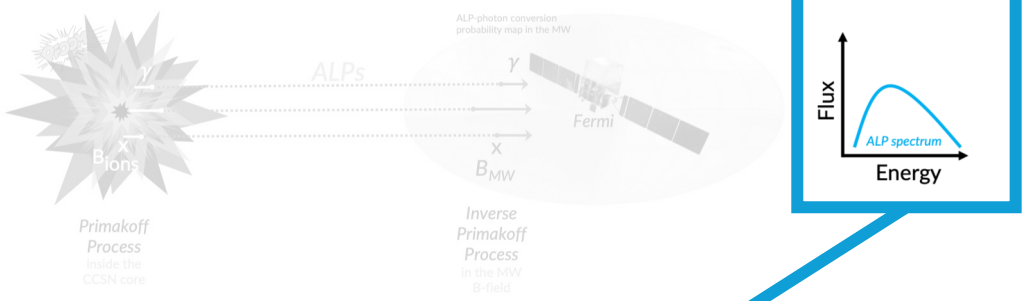

Motivation: ALPs are theorized to have a unique spectral signature in the prompt gamma-ray emission of CCSN. No other known physical processes are predicted to produce such a signature.

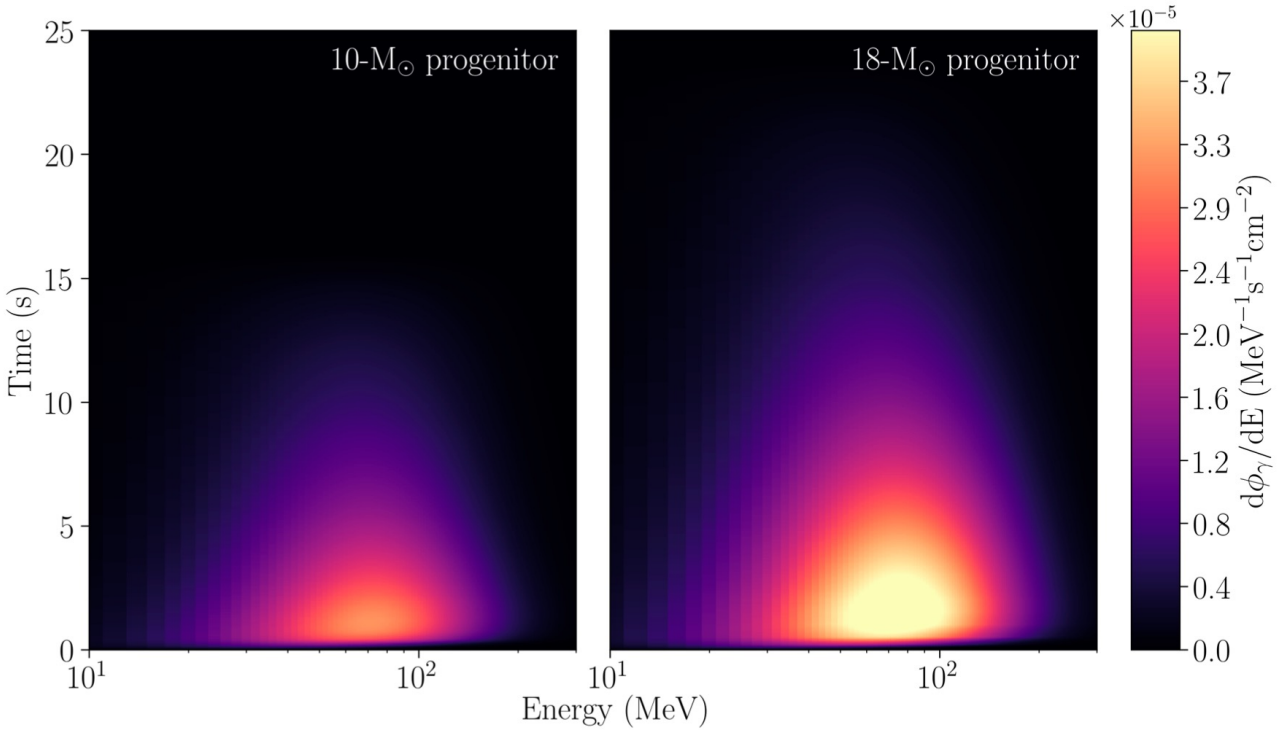

The observed evolution of the ALP-induced gamma-ray emission in time and energy in a core-collapse of a 10 and 18-$M_\odot$ progenitor.

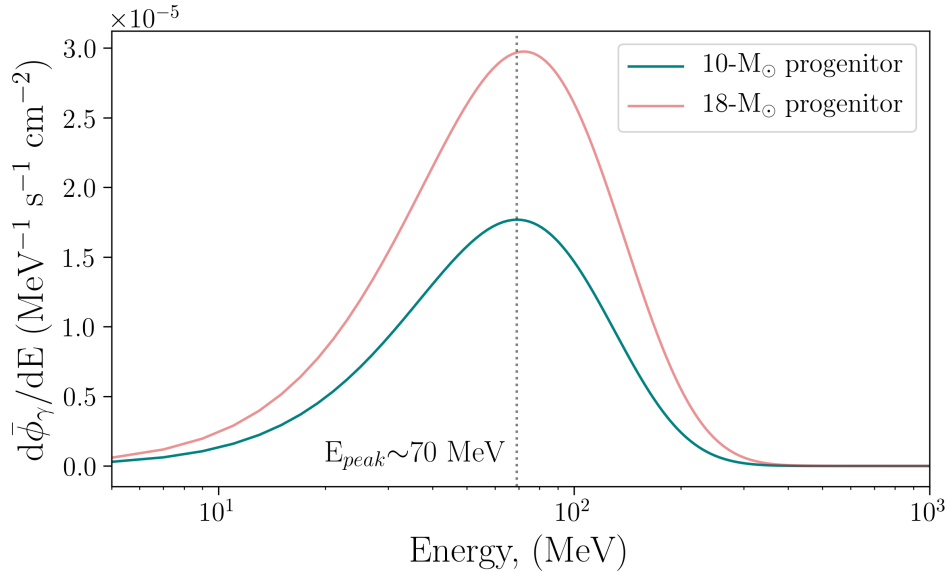

The observed ALP-induced gamma-ray spectrum for 10 and 18-$M_\odot$ progenitors averaged over 10 seconds.

The *Fermi*-LAT

e^+e^- pair-conversion telescope

individual γ rays convert into e^+e^- pairs
→ tracks (localization) & deposited energy

...it also detects electrons.

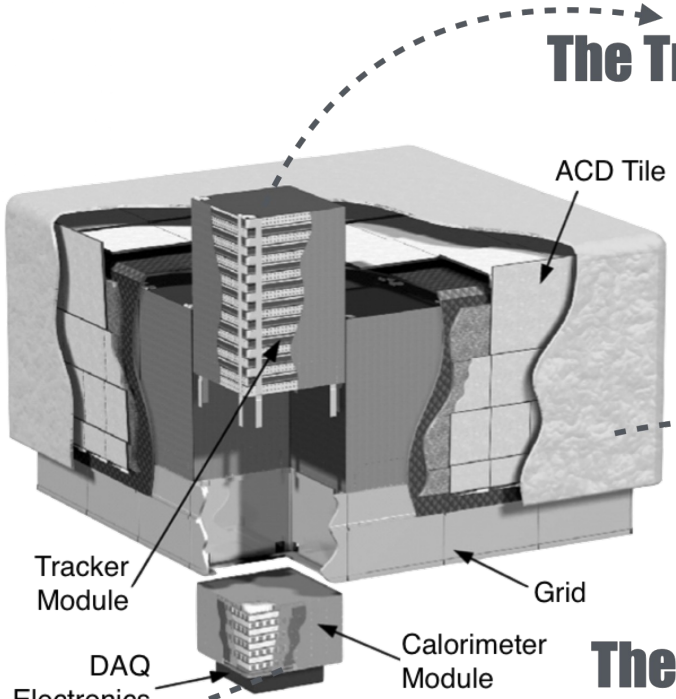

The *Fermi*-LAT

e^+e^- pair-conversion telescope

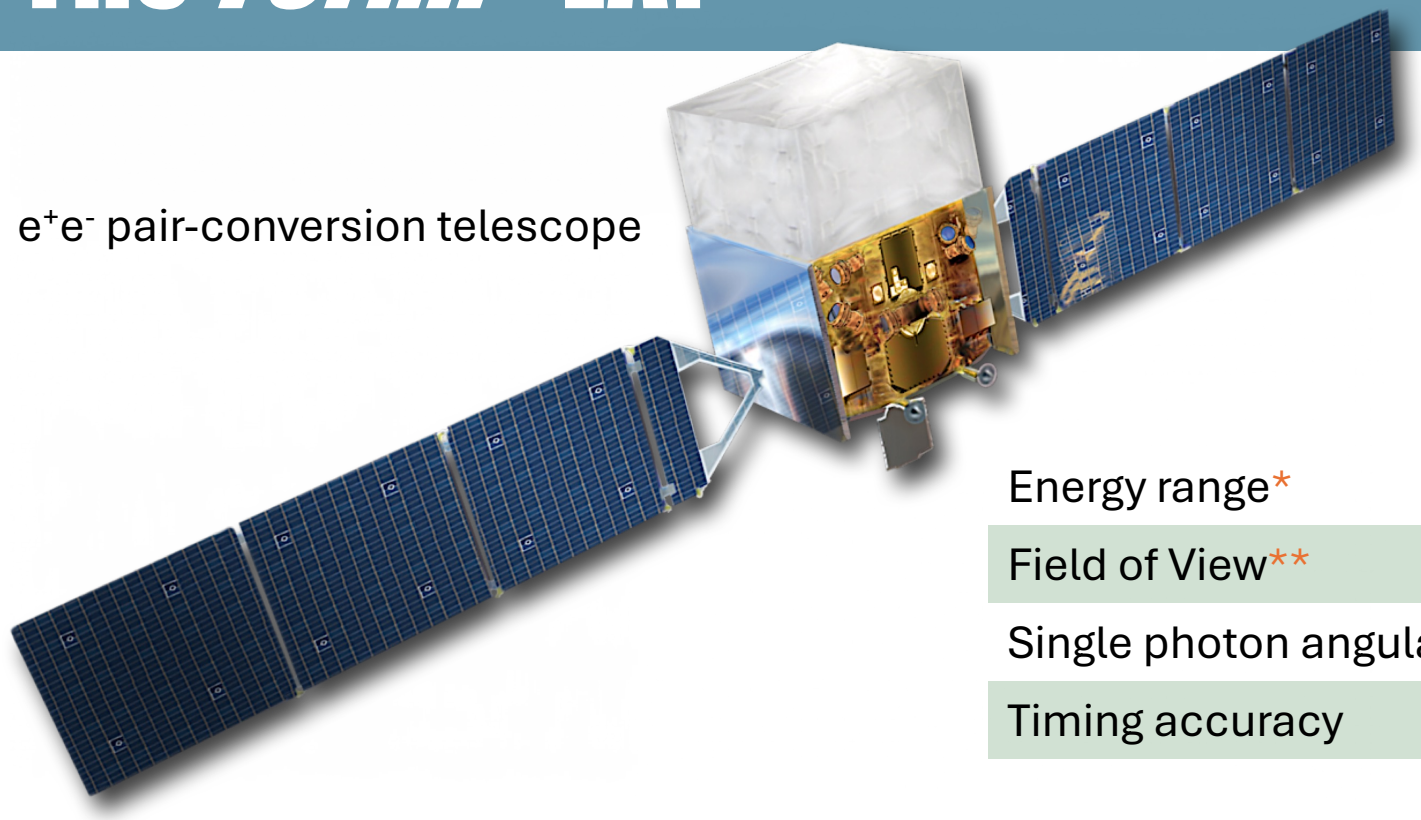

Energy range*	20 MeV to > 300 GeV
Field of View**	2.4 sr (~1/5 of the whole sky)
Single photon angular resolution***	< 1 deg at 1 GeV
Timing accuracy	1 microsecond

individual γ rays convert into e^+e^- pairs
→ tracks (localization) & deposited energy

*ideally suited for WIMP searches
**whole sky every ~3 hours
***point-source localization <0.5 arcmin

...it also detects electrons.

LAT Low Energy Technique (LLE)

ALP spectrum

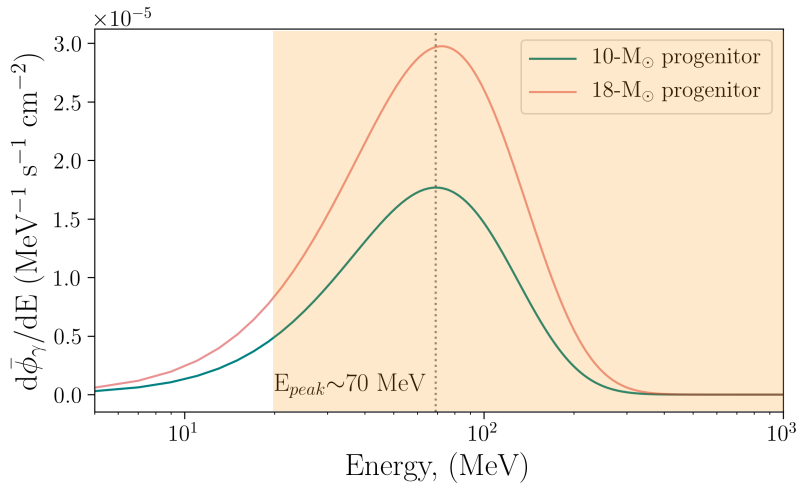

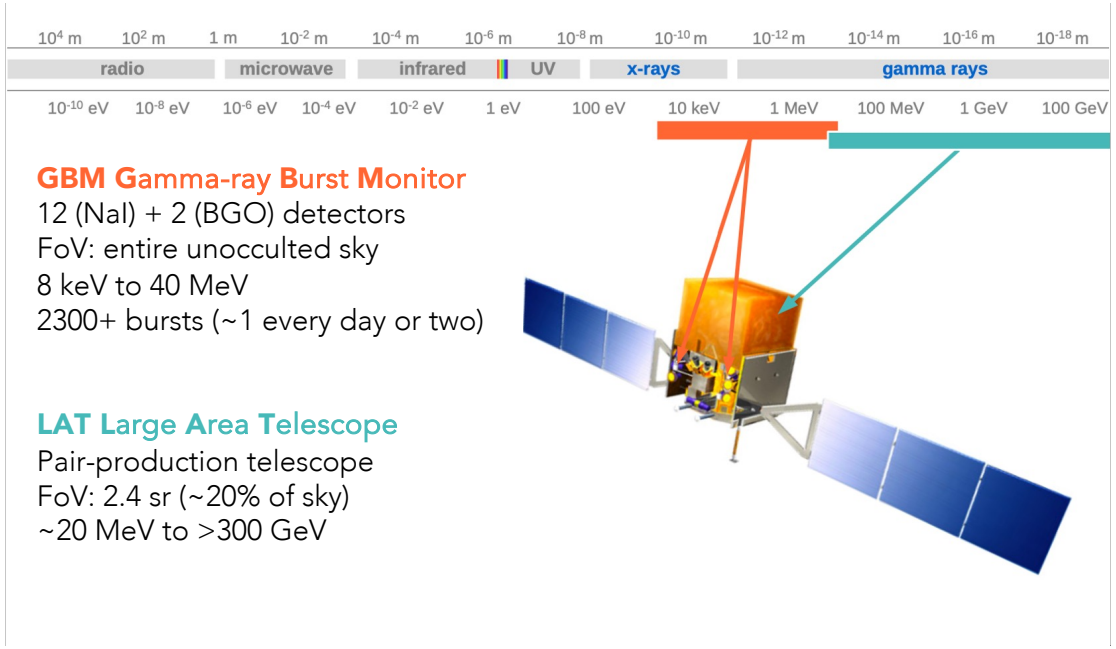

GBM Gamma-ray Burst Monitor
12 (NaI) + 2 (BGO) detectors
FoV: entire unocculted sky
8 keV to 40 MeV
2300+ bursts (~1 every day or two)

LAT Large Area Telescope
Pair-production telescope
FoV: 2.4 sr (~20% of sky)
~20 MeV to >300 GeV

- Standard LAT analysis: >100 MeV vs. LLE
- LLE: maximizing the effective area of the LAT instrument in the low-energy regime
- More signal, but also more background

LAT Low Energy Technique (LLE)

Light axionlike particles (ALPs) are expected to be abundantly produced in core-collapse supernovae (CCSNe), resulting in a ~10-second long burst of ALPs. These particles subsequently undergo conversion into gamma rays in external magnetic fields to produce a long gamma-ray burst (GRB) with a characteristic spectrum peaking in the 30–100-MeV energy range. At the same time, CCSNe are invoked as progenitors of *ordinary* long GRBs, rendering it relevant to conduct a comprehensive search for ALP spectral signatures using the observations of long GRBs with the *Fermi* Large Area Telescope (LAT). We perform a data-driven sensitivity analysis to determine CCSN distances for which a detection of an ALP signal is possible with the LAT's low-energy technique which, in contrast to the standard LAT analysis, allows for a a larger effective area for energies down to 30 MeV. Assuming an ALP mass $m_a \lesssim 10^{-10}$ eV and ALP-photon coupling $g_{a\gamma} = 5.3 \times 10^{-12}$ GeV^{-1}, values considered and deduced in ALP searches from SN1987A, we find that the distance limit ranges from ~0.5 to ~10 Mpc, depending on the sky location and the CCSN progenitor mass. Furthermore, we select a candidate sample of 24 GRBs and carry out a model comparison analysis in which we consider different GRB spectral models with and without an ALP signal component. We find that the inclusion of an ALP contribution does not result in any statistically significant improvement of the fits to the data. We discuss the statistical method used in our analysis and the underlying physical assumptions, the feasibility of setting upper limits on the ALP-photon coupling, and give an outlook on future telescopes in the context of ALP searches.

DOI: 10.1103/PhysRevD.104.103001

arXiv:2109.05790

- **Goal 1.** *Determining the sensitivity of LAT to detecting an ALP signal including energies below 100 MeV*

Result 1. *For representative ALP parameters (mass & coupling), LAT sensitivity to ALP signals from CCSNe are reached up to a distances of 10 Mpc.*

- **Goal 2.** *Determining whether an addition of an ALP model component improves the fit for a sample of unassociated, long, LLE-detected GRBs*

Result 2. *Including an additional ALP component does not result in a statistically significant model improvement for our GRB sample.*

Sensitivity testing: analysis and results

Model backgrounds from the considered LLE-detected GRB sample.

Find the min, max, and median background levels.

Produce ALP signal normalized by a value from the normalization grid for 10-and 18-solar-mass progenitors.

Produce 2000 realizations of the backround+ALP spectrum and their corresponding (GRB) response functions (XSPEC fakeit function.)

Fit the ALP and the "background-only" model. Apply Wilks' Theorem and LLR test to fins for which normalization ALP model is preferred.

Find the coupling-distance parameter space for that normalization.

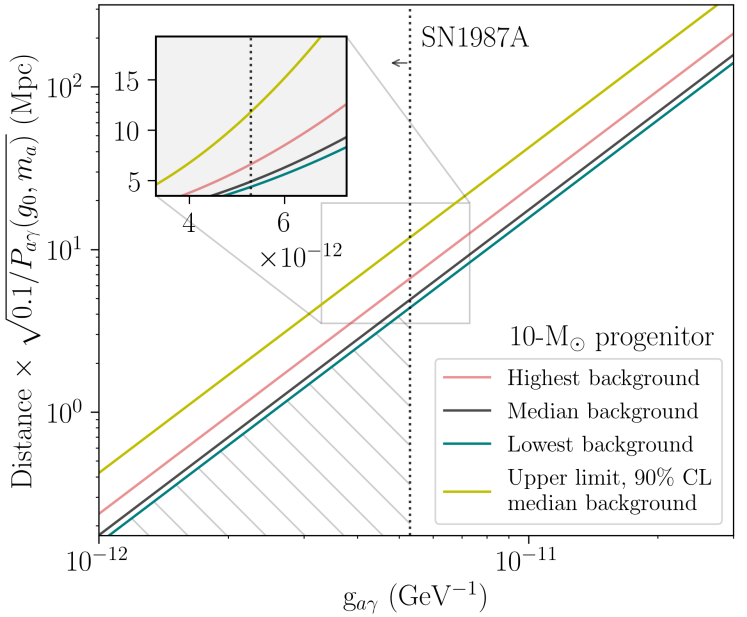

Background level	Conversion probability, $P_\gamma(g_0)$	Distance limit (Mpc) 10 M$_\odot$	18 M$_\odot$
Low	0.1	4.4	6.5
Median	0.1	4.9	7.1
High	0.1	6.6	9.7
Low	0.05	3.1	4.6
Median	0.05	3.5	5.0
High	0.05	4.7	6.9
Low	0.01	1.4	2.1
Median	0.01	1.5	2.3
High	0.01	2.1	3.1
Low	0.001	0.4	0.7
Median	0.001	0.5	0.7
High	0.001	0.7	1.0

Sensitivity testing: analysis and results

Model backgrounds from the considered LLE-detected GRB sample.

Find the min, max, and median background levels.

Produce ALP signal normalized by a value from the normalization grid for 10-and 18-solar-mass progenitors.

Produce 2000 realizations of the backround+ALP spectrum and their corresponding (GRB) response functions (XSPEC fakeit function.)

Fit the ALP and the "background-only" model. Apply Wilks' Theorem and LLR test to fins for which normalization ALP model is preferred.

Find the coupling-distance parameter space for that normalization.

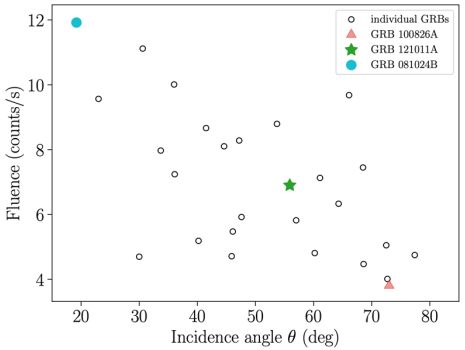

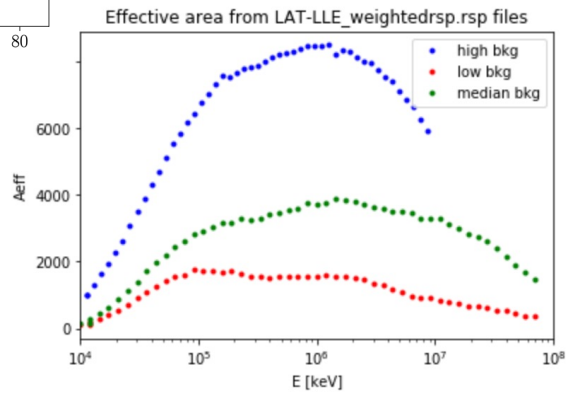

Background level	Conversion probability, $P_\gamma(g_0)$	Distance limit (Mpc) 10 $M_\odot$	18 $M_\odot$
Low	0.1	4.4	6.5
Median	0.1	4.9	7.1
High	0.1	6.6	9.7
Low	0.05	3.1	4.6
Median	0.05	3.5	5.0
High	0.05	4.7	6.9
Low	0.01	1.4	2.1
Median	0.01	1.5	2.3
High	0.01	2.1	3.1
Low	0.001	0.4	0.7
Median	0.001	0.5	0.7
High	0.001	0.7	1.0

HAVE WE ALREADY SEEN ANY ALP EMISSION IN LLE GRBS?

Reported in: Crnogorčević et al. 2021 (PRD, arXiv:2109.05790)

GRB Analysis Results

Property	Selection Criterion
Distance	unassociated (no redshift)
Detection significance	$\geq 5\sigma$ in LAT-LLE ($\gtrsim 30$ MeV)
Observed time interval	$\geq$ duration of the burst
Burst duration	long GRBs ($T_{95} \gtrsim 2$ seconds) *(not used in Sec. IV)*

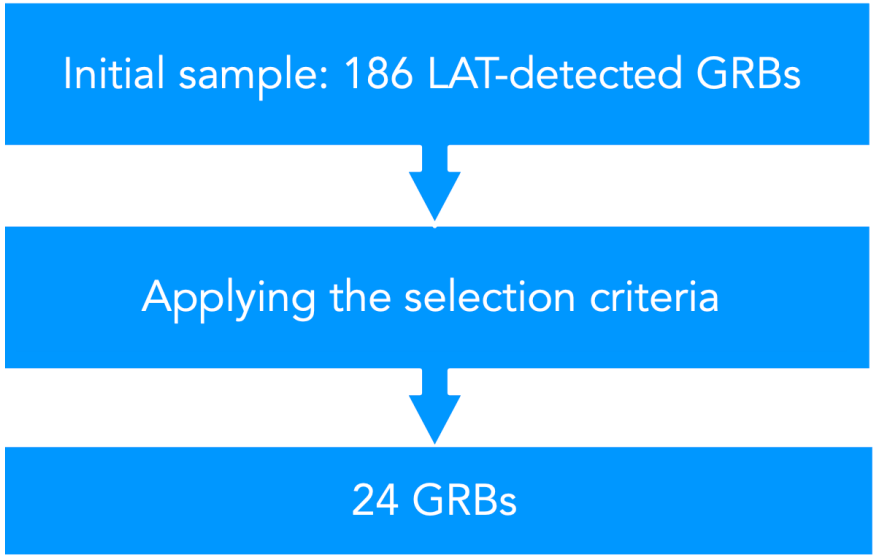

GRB Analysis Results

GRB	T_{95} (s)	Best model(no ALP)	grbm parameters			LLR
			α_1	α_2	E_c (keV)	
080825C	22.2	grbm	$-0.65^{+0.05}_{-0.05}$	$-2.41^{+0.04}_{-0.04}$	143^{+13}_{-12}	0.2
090217	34.1	grbm	$-1.11^{+0.04}_{-0.04}$	$-2.43^{+0.03}_{-0.04}$	16^{+13}_{-8}	0.1
100225A	12.7	grbm	$-0.50^{+0.25}_{-0.21}$	$-2.28^{+0.07}_{-0.09}$	223^{+112}_{-68}	0.0
100826A	93.7	grbm+bb	$-1.02^{+0.04}_{-0.04}$	$-2.30^{+0.03}_{-0.04}$	484^{+72}_{-63}	0.0
101123A	145.4	grbm+cutoffpl	$-1.00^{+0.07}_{-0.08}$	$-1.94^{+0.15}_{-0.12}$	187^{+74}_{-62}	5.8
110721A	21.8	grbm+bb	$-1.24^{+0.02}_{-0.01}$	$-2.29^{+0.03}_{-0.03}$	1000^{+28}_{-39}	0.0
120328B	33.5	grbm+cutoffpl	$-0.67^{+0.06}_{-0.05}$	$-2.26^{+0.05}_{-0.05}$	101^{+12}_{-13}	0.0
120911B	69.0	grbm	$-2.50^{+0.92}_{-1.04}$	$-1.05^{+0.63}_{-0.38}$	11^{+10}_{-2}	0.0
121011A	66.8	grbm	$-1.08^{+0.10}_{-0.21}$	$-2.18^{+0.11}_{-0.16}$	997^{+84}_{-26}	0.0
121225B	68.0	grbm	$-2.38^{+1.02}_{-0.40}$	$-2.45^{+0.06}_{-0.07}$	11^{+89}_{-3}	0.0
130305A	26.9	grbm	$-0.76^{+0.03}_{-0.03}$	$-2.63^{+0.06}_{-0.06}$	665^{+61}_{-55}	0.0
131014A	4.2	grbm	$-0.55^{+0.33}_{-0.98}$	$-2.65^{+0.17}_{-0.19}$	255^{+36}_{-11}	0.63
131216A	19.3	grbm+cutoffpl	$-0.46^{+0.28}_{-0.24}$	$-2.67^{+1.94}_{-0.94}$	178^{+77}_{-92}	0.0
140102A	4.1	grbm+bb	$-1.10^{+0.12}_{-0.09}$	$-2.41^{+0.16}_{-0.11}$	206^{+65}_{-92}	2.3
140110A	9.2	grbm	$-2.49^{+1.64}_{-1.59}$	$-2.19^{+0.20}_{-0.22}$	11^{+23}_{-3}	0.0
141207A	22.3	grbm+bb	$-1.21^{+0.09}_{-0.06}$	$-2.33^{+0.11}_{-0.13}$	999^{+18}_{-70}	0.0
141222A	2.8	grbm+pow	$-1.57^{+0.03}_{-0.02}$	$-2.83^{+0.46}_{-1.74}$	9971^{+390}_{-832}	0.0
150210A	31.3	grbm+pow	$-0.52^{+0.04}_{-0.05}$	$-2.91^{+0.11}_{-0.38}$	1000^{+517}_{-234}	0.0
150416A	33.8	grbm	$-1.18^{+0.04}_{-0.04}$	$-2.36^{+0.13}_{-0.21}$	999^{+187}_{-269}	0.0
150820A	5.1	grbm	$-0.99^{+0.56}_{-1.30}$	$-2.01^{+0.82}_{-0.27}$	303^{+61}_{-39}	0.0
151006A	95.0	grbm	$-1.35^{+0.06}_{-0.03}$	$-2.24^{+0.07}_{-0.08}$	998^{+33}_{-84}	0.0
160709A	5.4	grbm+cutoffpl	$-1.44^{+0.18}_{-0.12}$	$-2.18^{+0.15}_{-0.18}$	9940^{+373}_{-511}	1.0
160917A	19.2	grbm+bb	$-0.78^{+3.45}_{-1.40}$	$-2.39^{+0.20}_{-0.10}$	994^{+634}_{-216}	0.9
170115B	44.8	grbm	$-0.80^{+0.02}_{-0.04}$	$-3.00^{+0.10}_{-0.07}$	1000^{+226}_{-106}	2.8

GRB Analysis Results

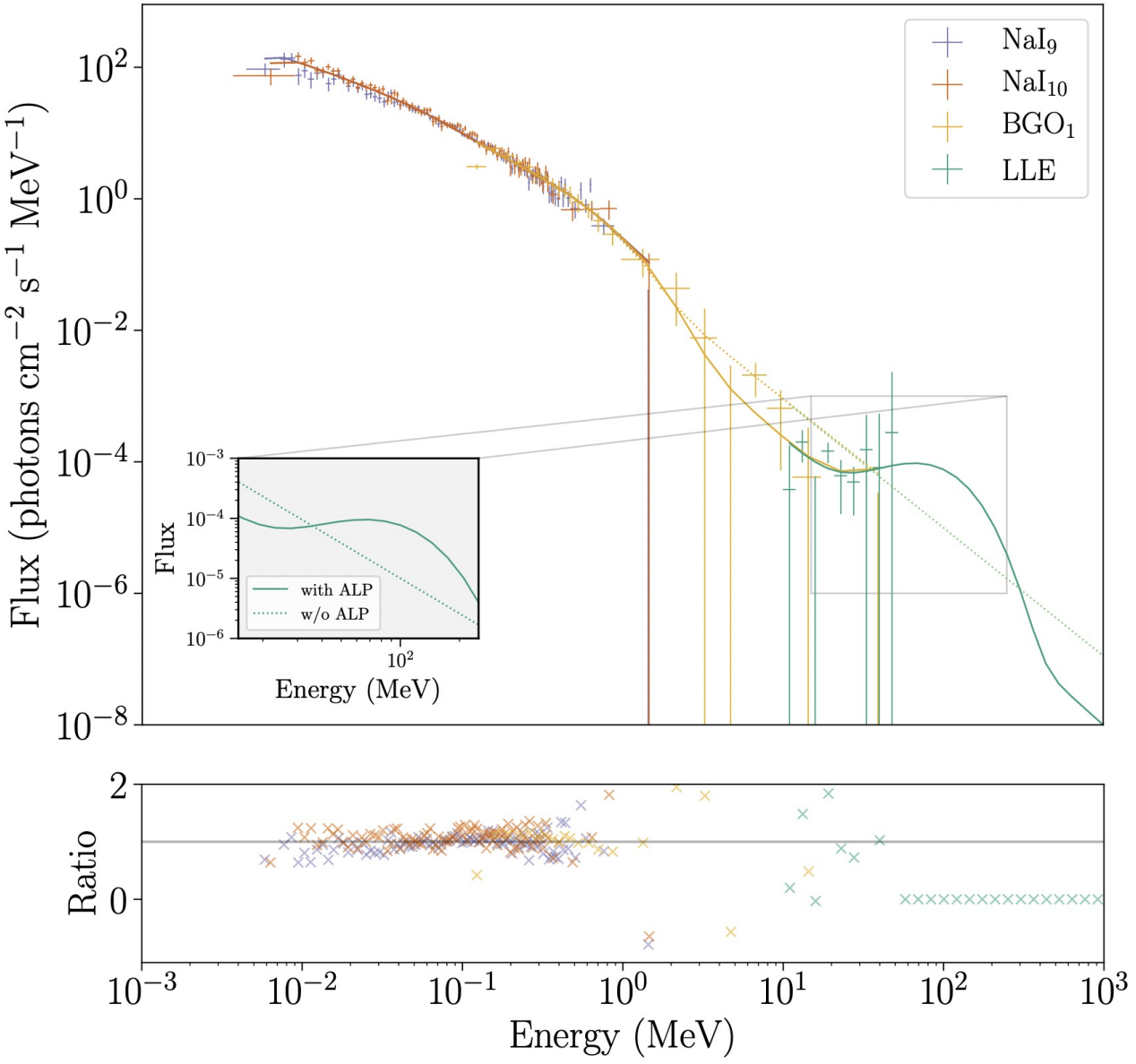

global p-value of ~0.3, indicating that this observation is not statistically significant.

WHEN SHOULD WE SEARCH FOR ALPS FROM GRBS?

Fermi GI Program, Cycle 15; PI: Crnogorčević

Reported in: Crnogorčević et al. 2024 (in prep.)

GRB lightcurve

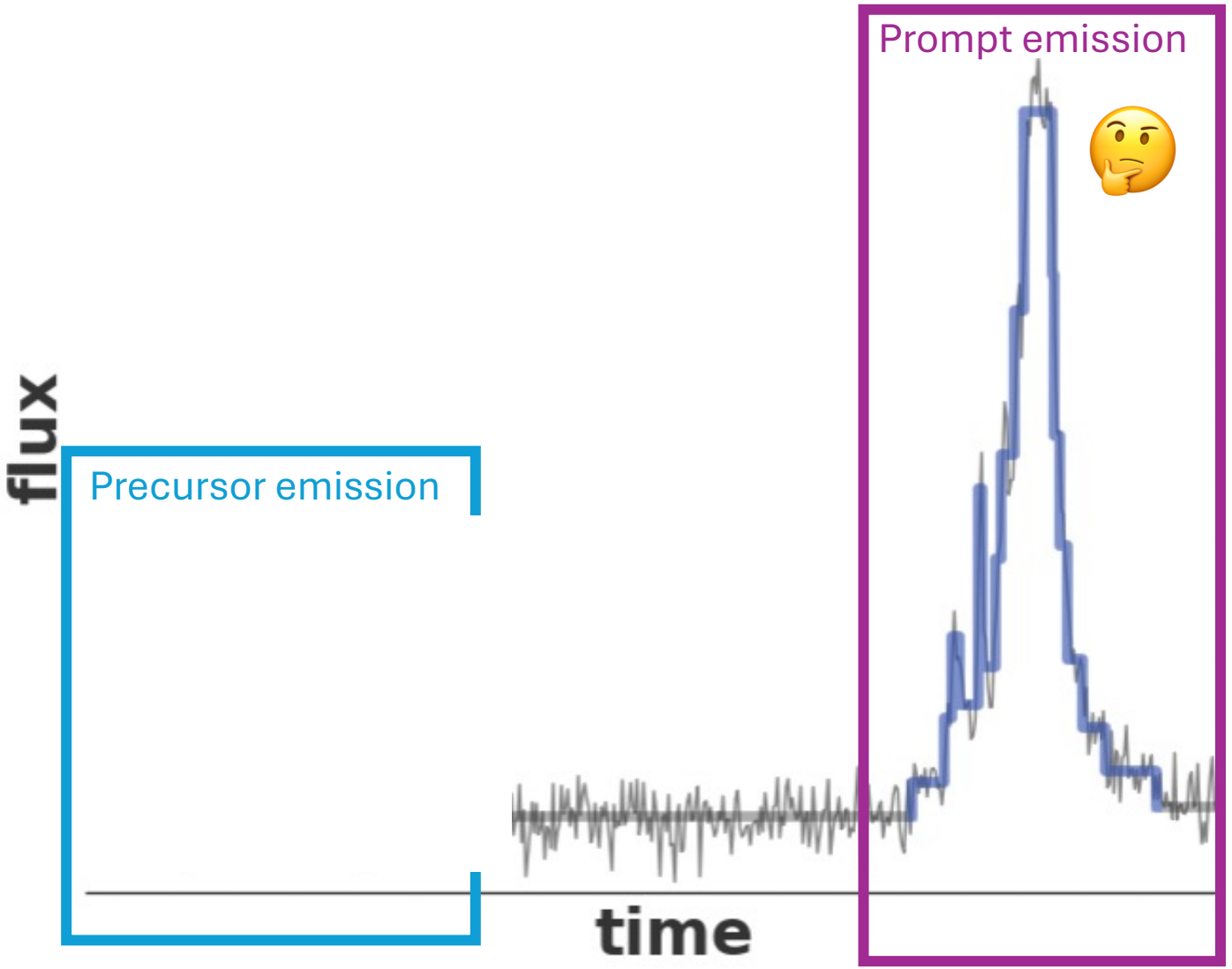

Precursors may come from…

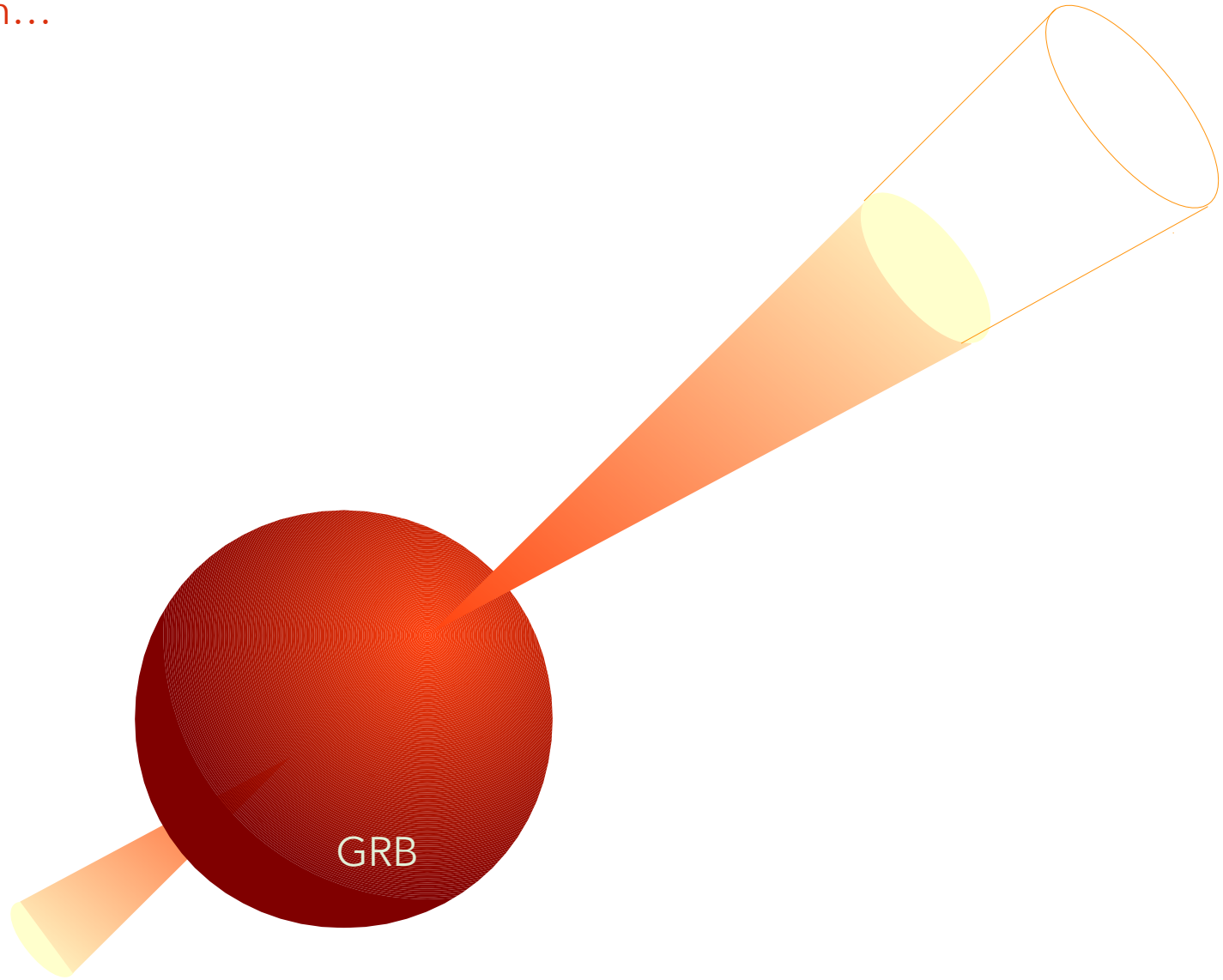

Diagram adapted from Sylvia Zhu's dissertation

Precursors may come from…

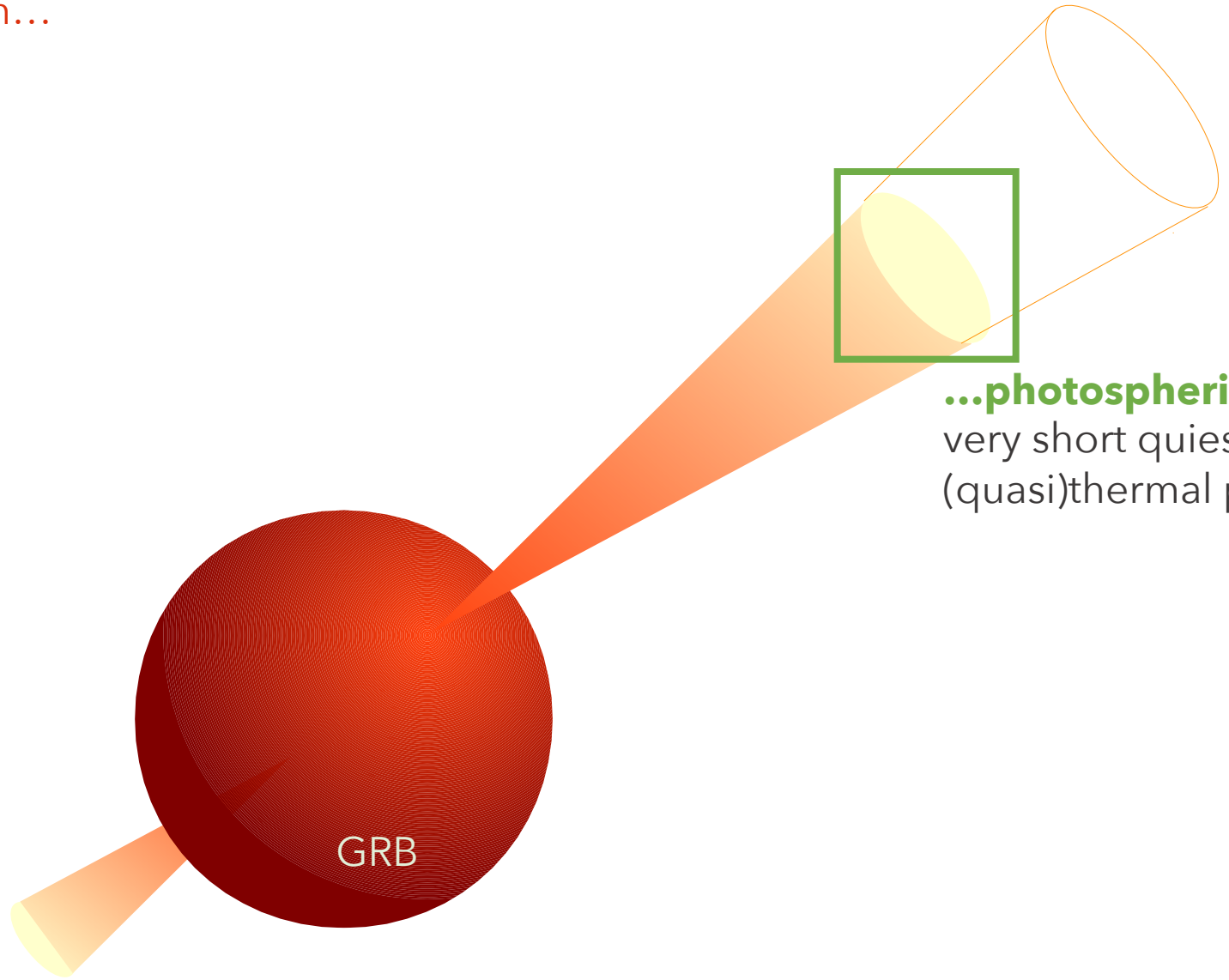

…photospheric emission
very short quiescent periods
(quasi)thermal precursor

Diagram adapted from Sylvia Zhu's dissertation

Precursors may come from…

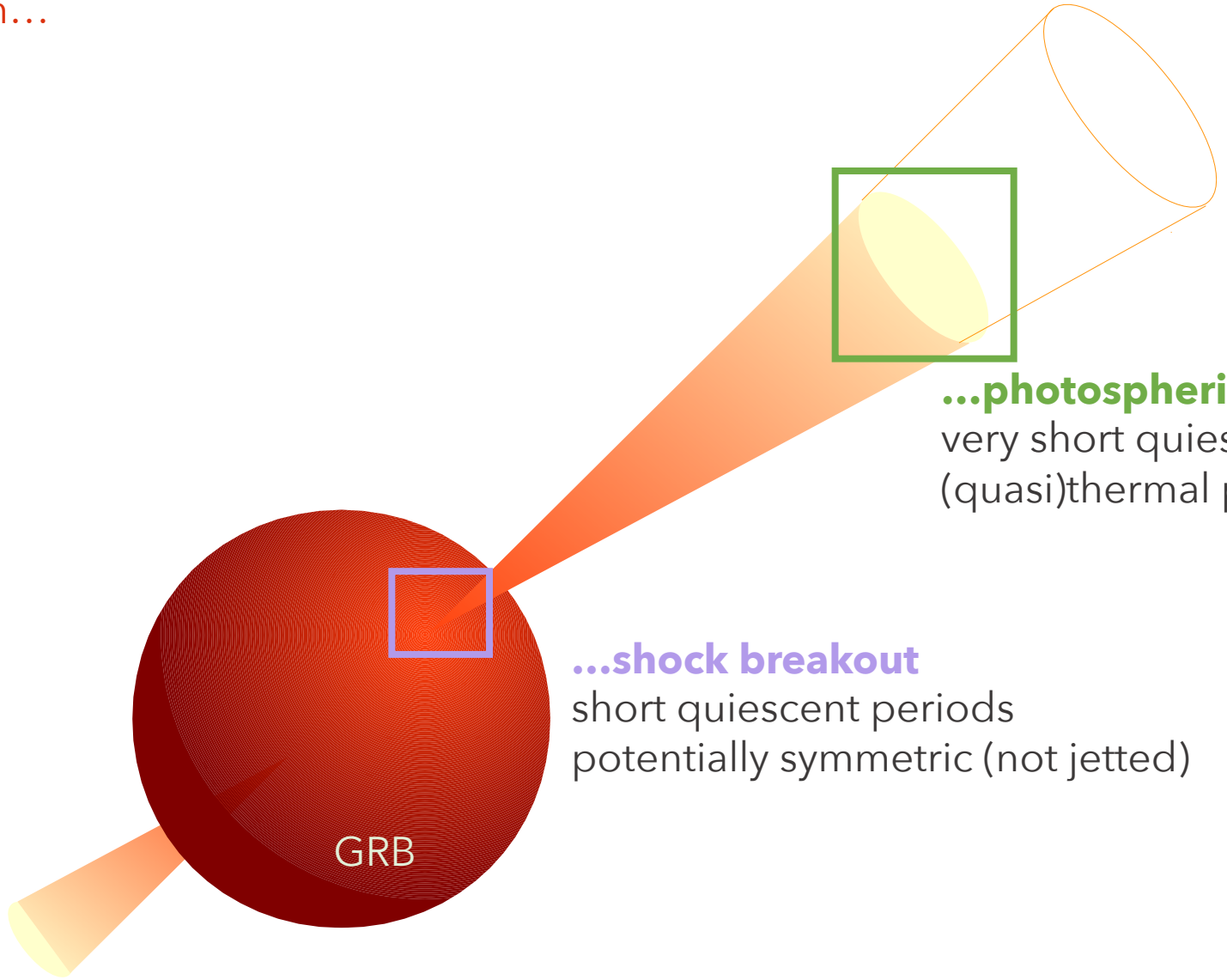

…photospheric emission
very short quiescent periods
(quasi)thermal precursor

…shock breakout
short quiescent periods
potentially symmetric (not jetted)

Diagram adapted from Sylvia Zhu's dissertation

Precursors may come from…

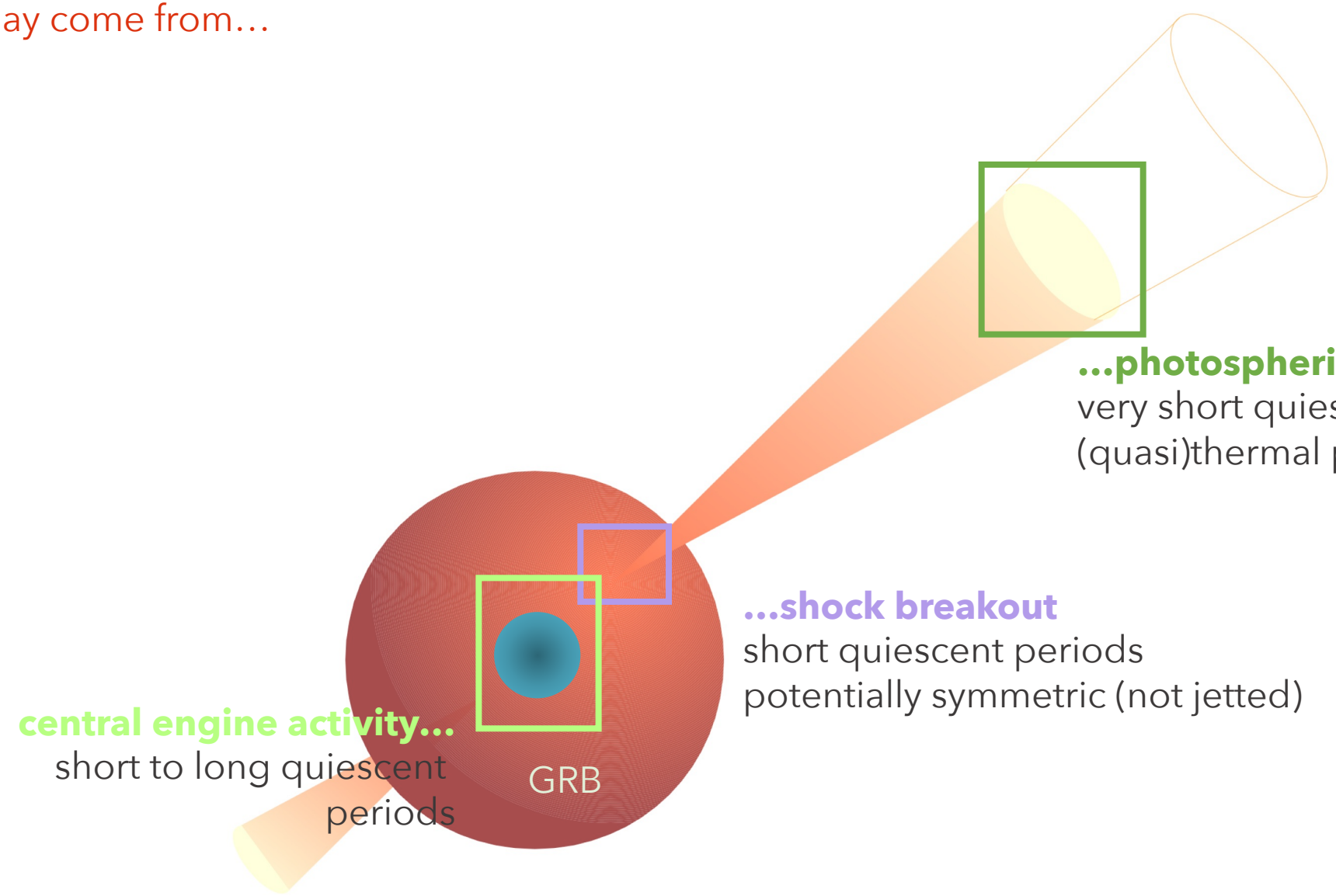

…photospheric emission
very short quiescent periods
(quasi)thermal precursor

…shock breakout
short quiescent periods
potentially symmetric (not jetted)

central engine activity…
short to long quiescent periods

Diagram adapted from Sylvia Zhu's dissertation

Precursors may come from…

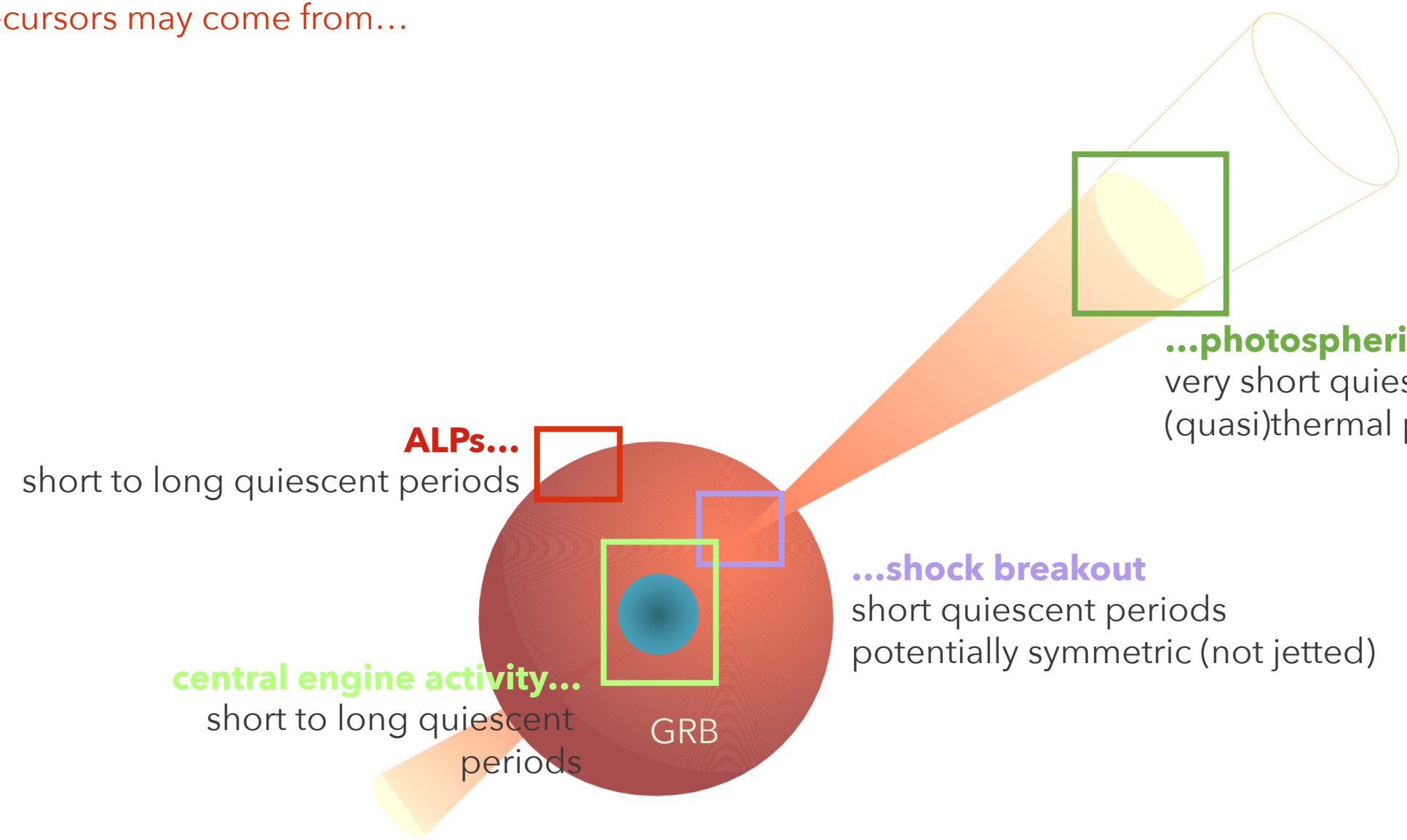

Diagram adapted from Sylvia Zhu's dissertation

Time-resolved analysis

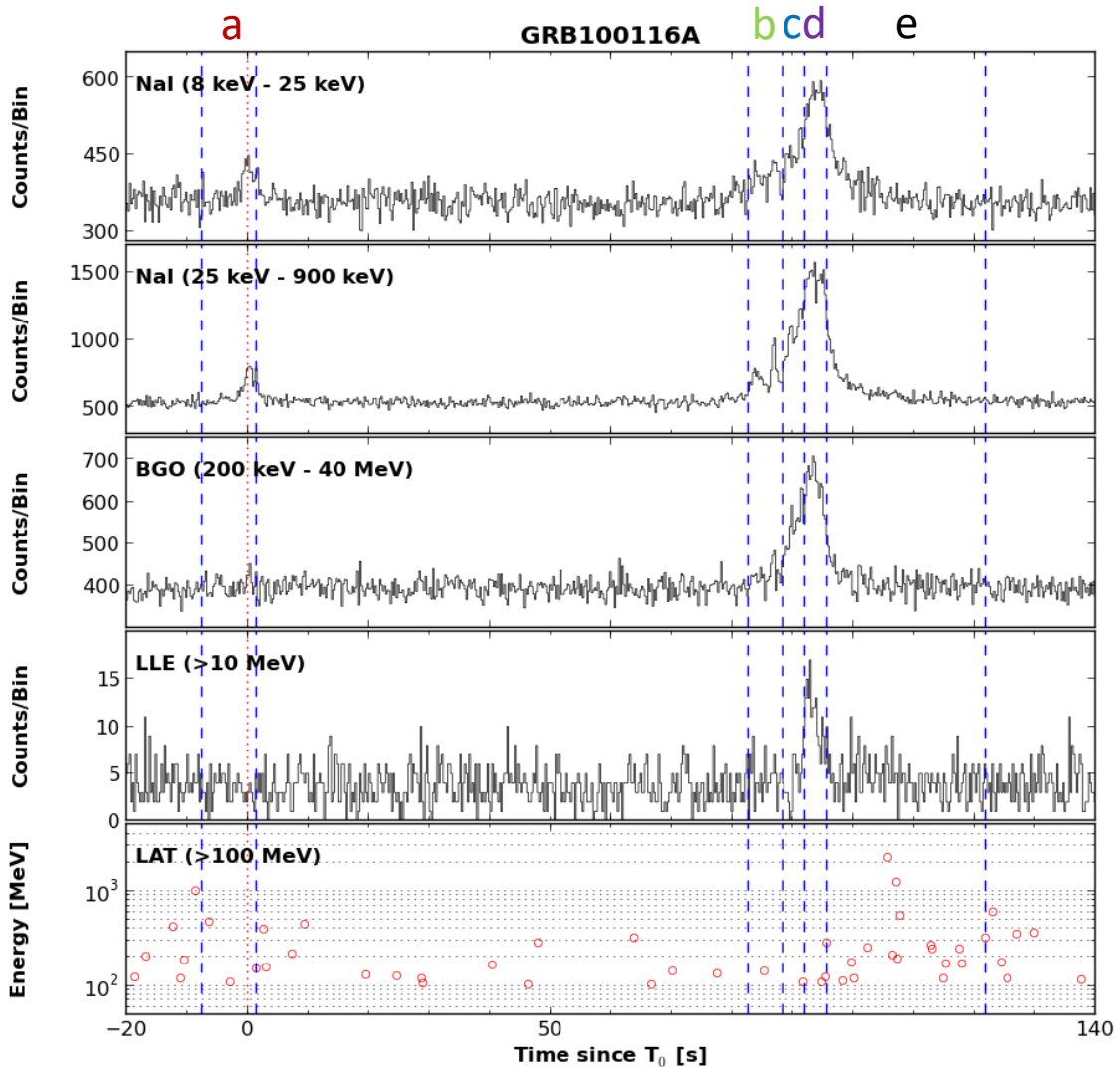

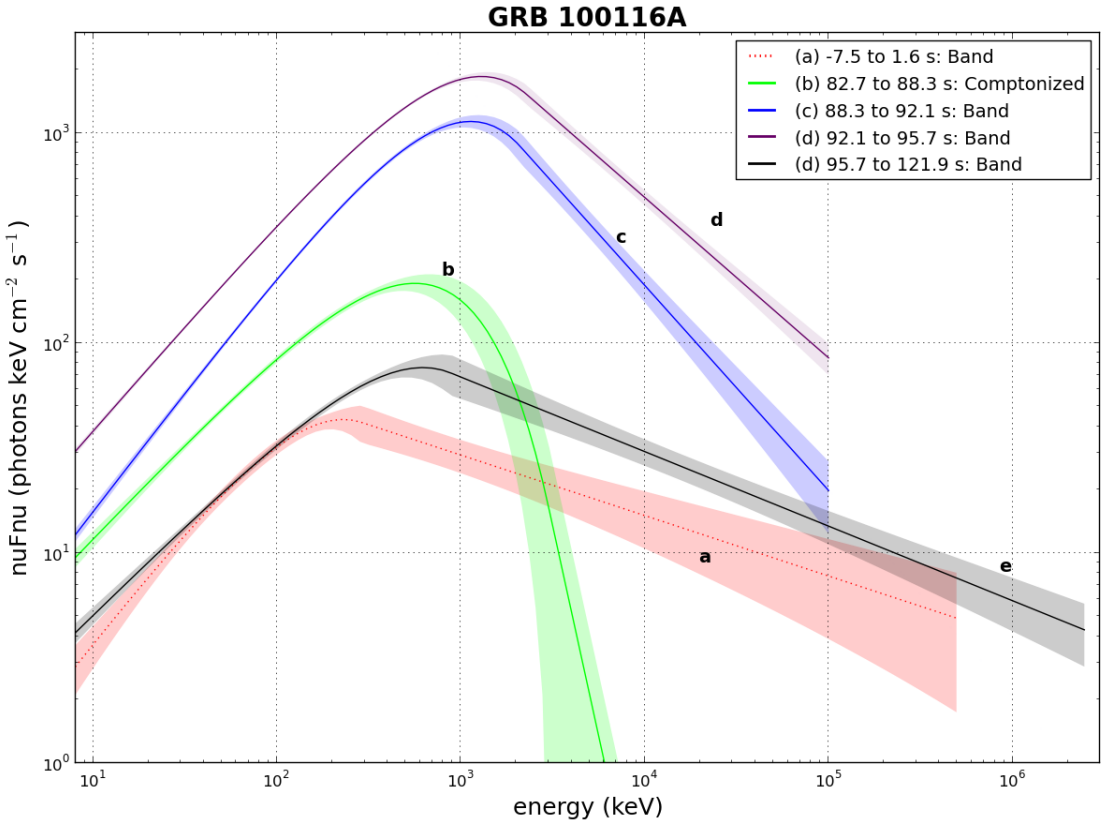

GRB analysis

Property	Selection Criterion
Observed time interval	inside LAT FoV for ~1000 s prior to the trigger time T_0
Burst duration	long GRBs ($T_{90} \gtrsim 2$ seconds)
Precursor confirmed	`BB algorithm` (see 4.4.1)
GBM precursor	no temporal coincidence

?

(interesting analysis can be done, but not in this context, ~20% of bursts w/ precursor)

Initial sample: 255 GRBs (LAT/LLE)

Applying the selection criteria

14 GRBs in LAT and 7 in LLE (3 overlap)

Best

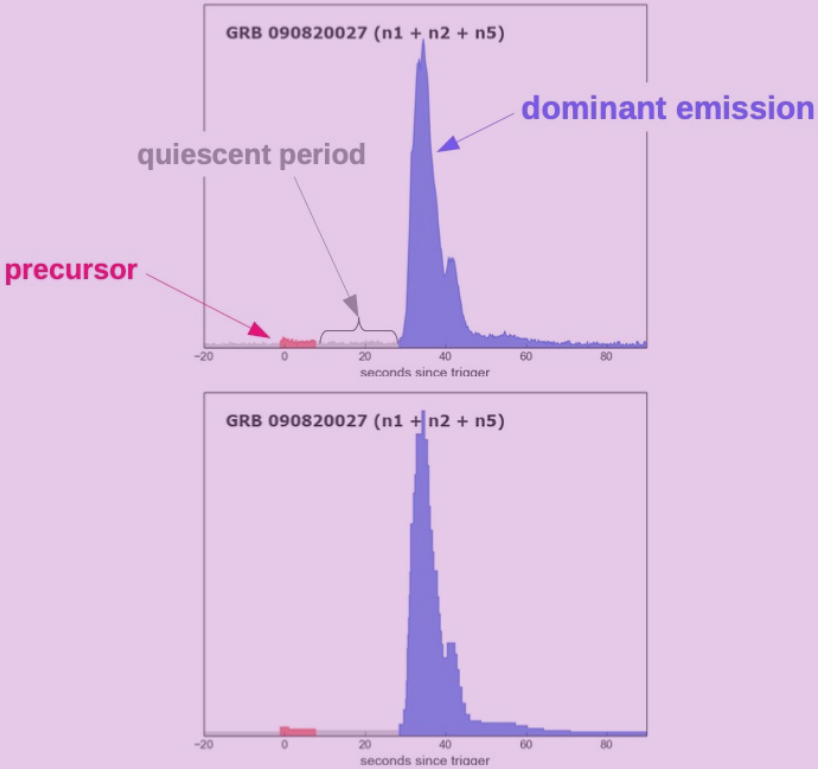
GRB 090820027 (n1 + n2 + n5)
dominant emission
quiescent period
precursor
seconds since trigger
GRB 090820027 (n1 + n2 + n5)
seconds since trigger

Good

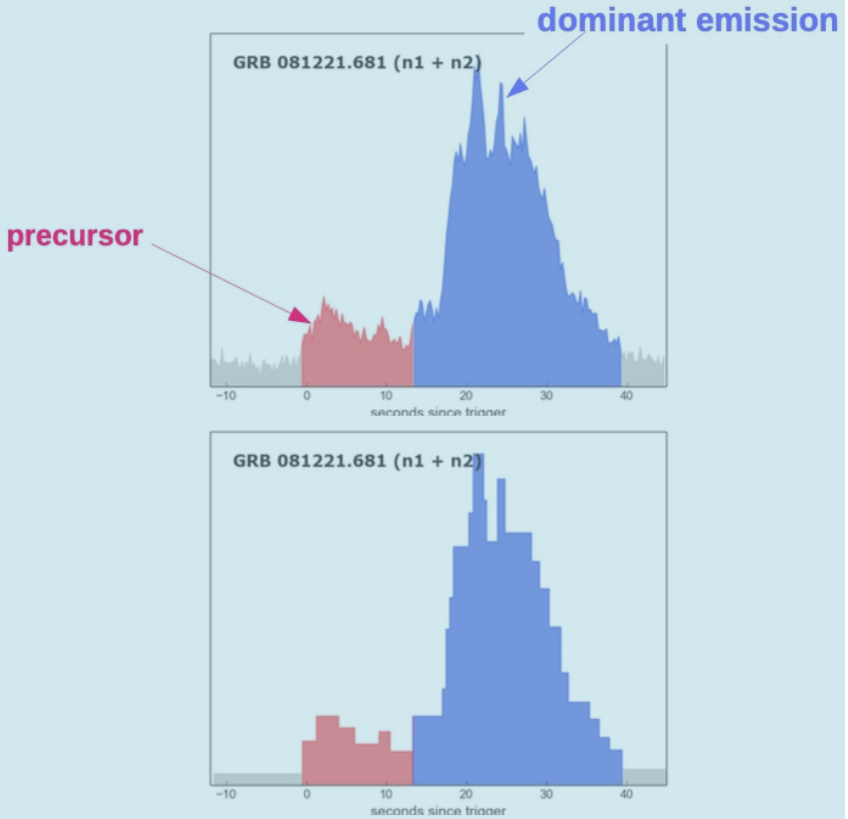
dominant emission
GRB 081221.681 (n1 + n2)
precursor
seconds since trigger
GRB 081221.681 (n1 + n2)
seconds since trigger

🤷‍♀️

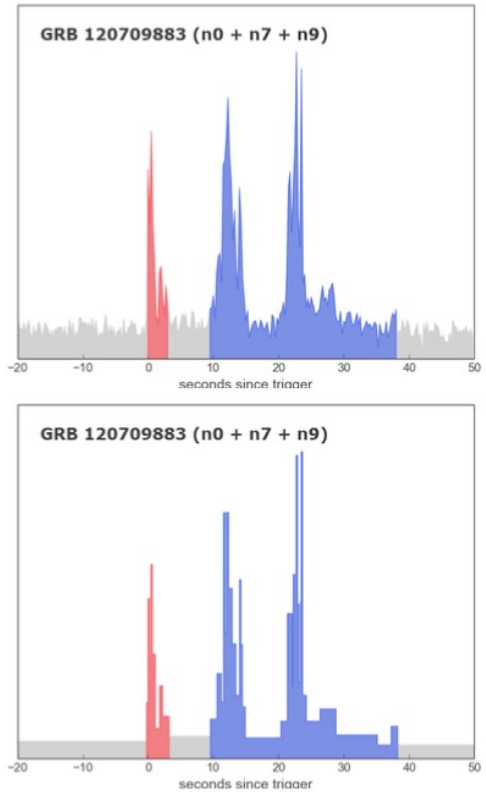
GRB 120709883 (n0 + n7 + n9)
seconds since trigger
GRB 120709883 (n0 + n7 + n9)
seconds since trigger

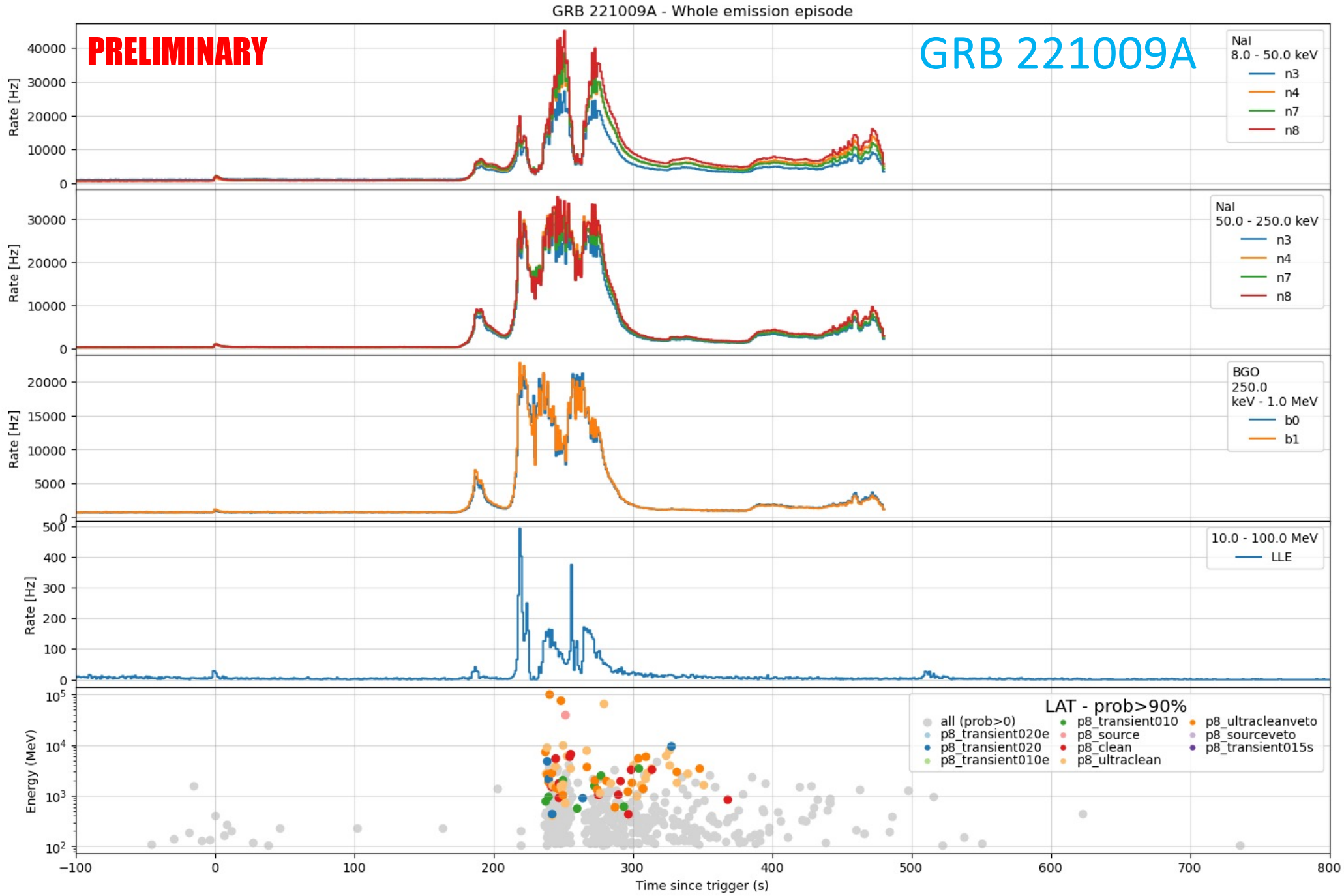
GRB 221009A - Whole emission episode
PRELIMINARY
GRB 221009A
NaI
8.0 - 50.0 keV
n3
n4
n7
n8
NaI
50.0 - 250.0 keV
n3
n4
n7
n8
BGO
250.0
keV - 1.0 MeV
b0
b1
10.0 - 100.0 MeV
LLE
LAT - prob>90%
all (prob>0)
p8_transient020e
p8_transient020
p8_transient010e
p8_transient010
p8_source
p8_clean
p8_ultraclean
p8_ultracleanveto
p8_sourceveto
p8_transient015s
Rate [Hz]
Energy (MeV)
Time since trigger (s)

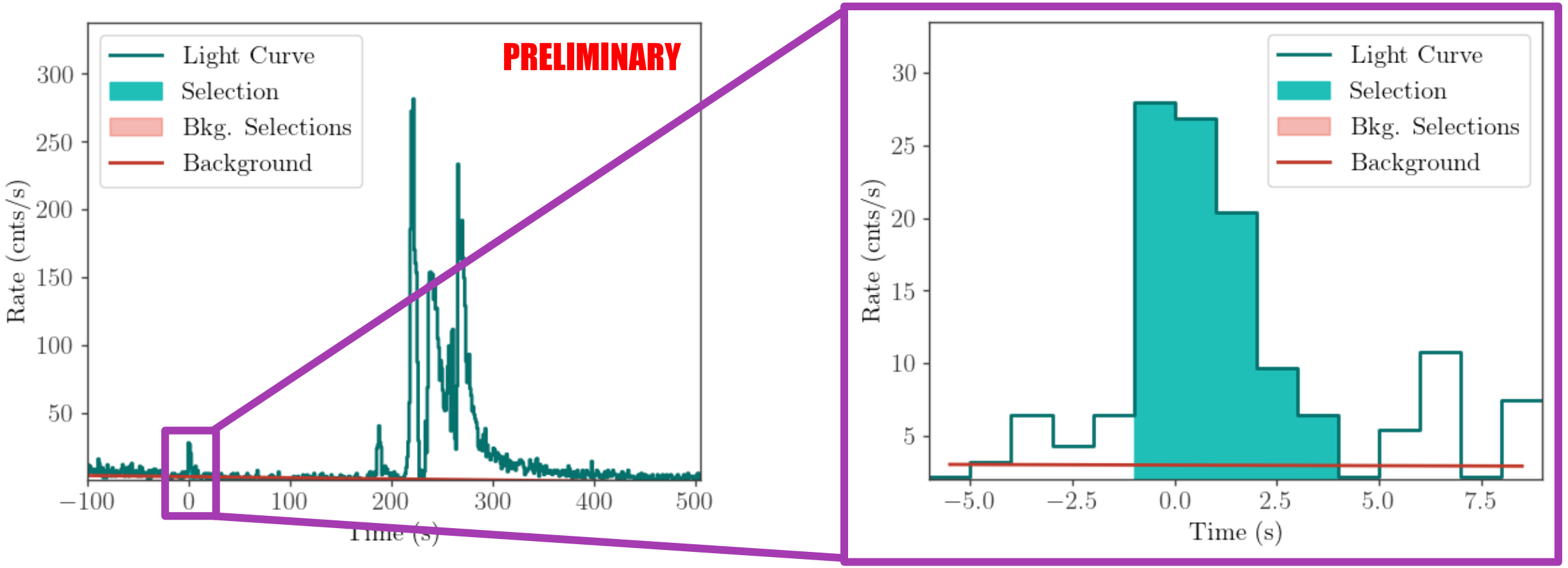
PRELIMINARY
Light Curve
Selection
Bkg. Selections
Background
Rate (cnts/s)
Time (s)
300
250
200
150
100
50
−100
0
100
200
300
400
500
30
25
20
15
10
5
−5.0
−2.5
0.0
2.5
5.0
7.5

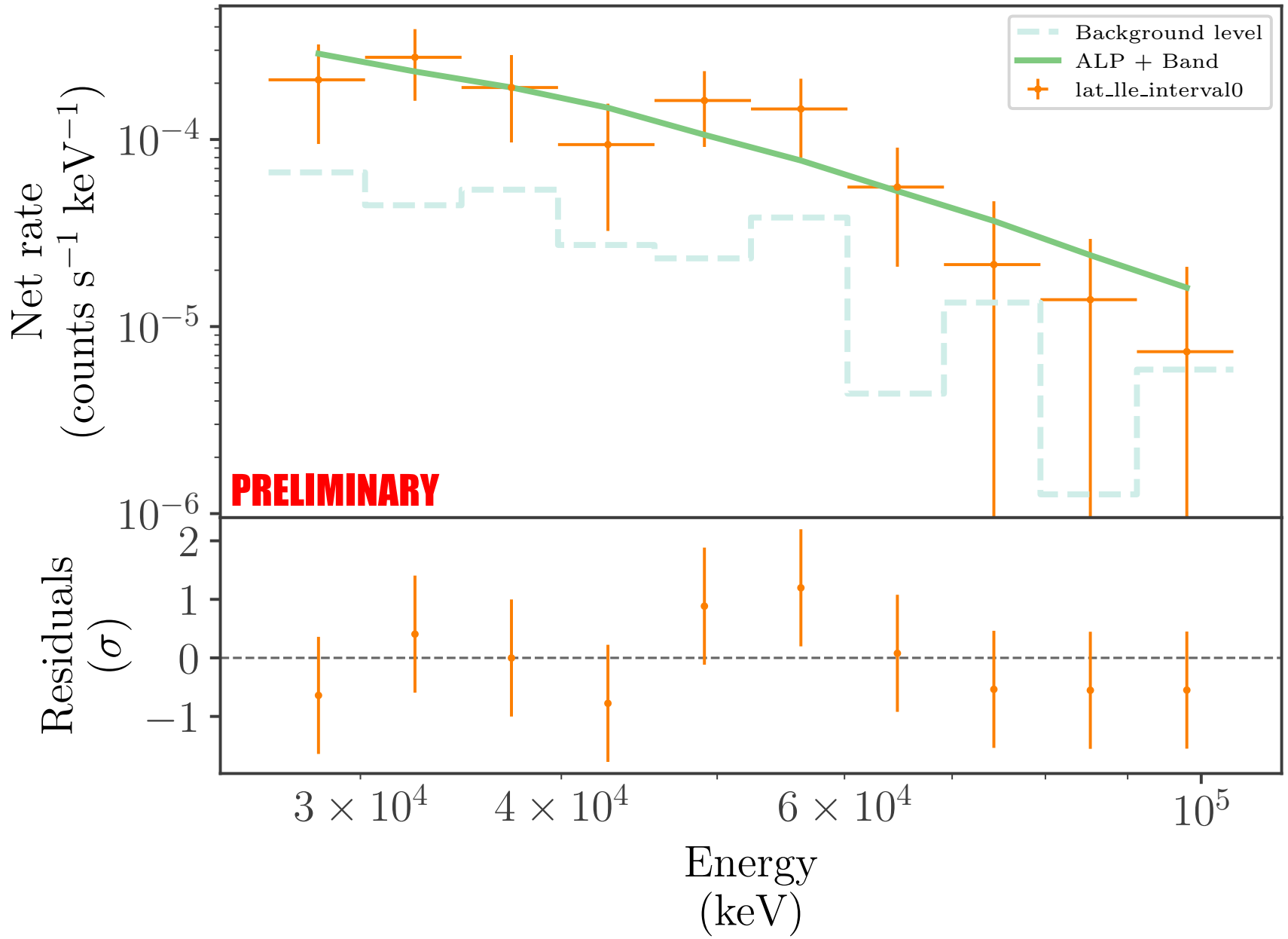
Background level
ALP + Band
lat_lle_interval0
PRELIMINARY
Net rate
(counts s^{-1} keV^{-1})
10^{-4}
10^{-5}
10^{-6}
Residuals
(σ)
2
1
0
−1
3×10^4
4×10^4
6×10^4
10^5
Energy
(keV)

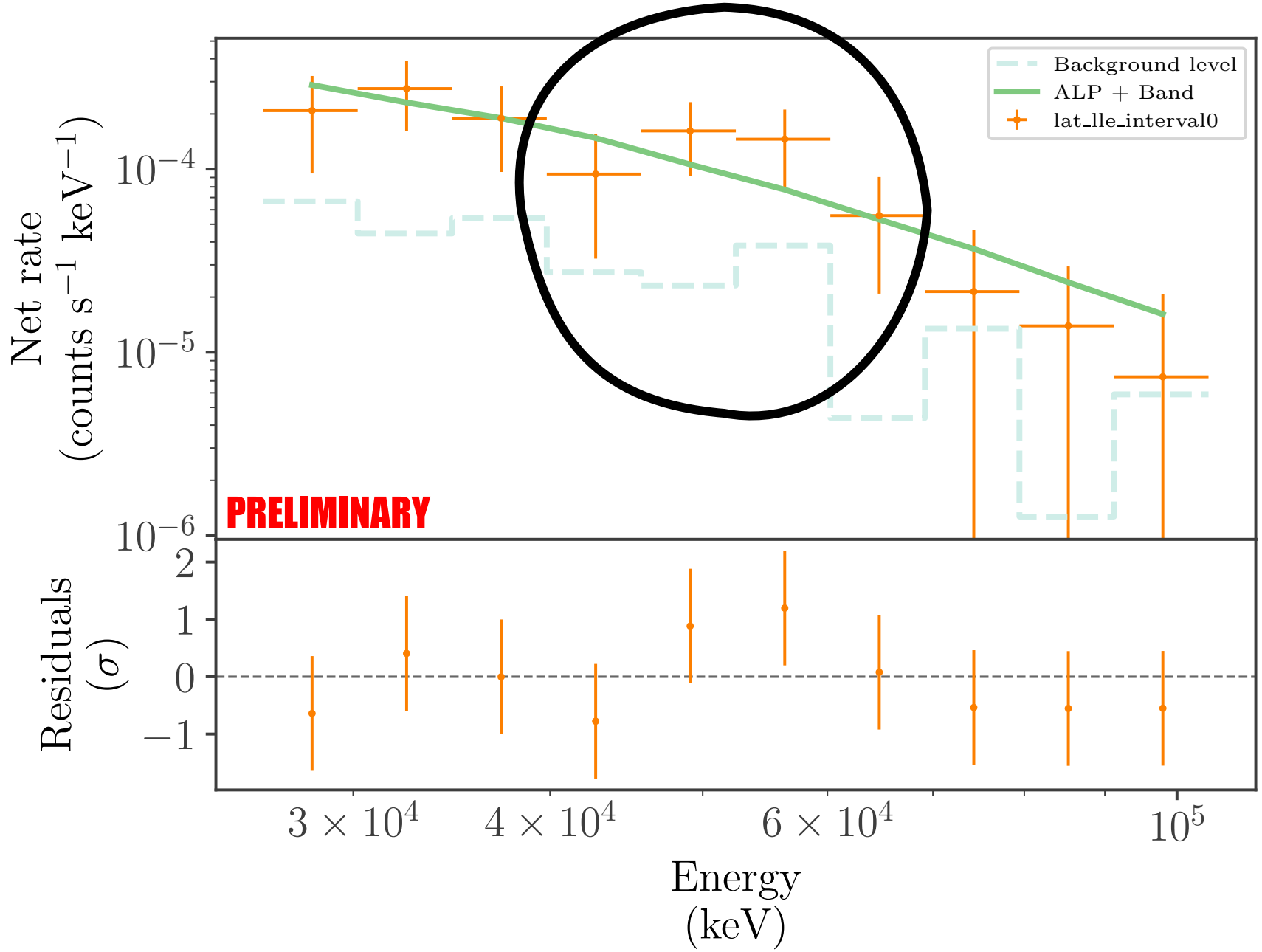
Background level
ALP + Band
lat_lle_interval0
PRELIMINARY
Net rate
(counts s^{-1} keV^{-1})
10^{-4}
10^{-5}
10^{-6}
Residuals
(σ)
2
1
0
−1
3×10^4
4×10^4
6×10^4
10^5
Energy
(keV)

GRB Name	T_0 (MET)	Precursor w.r.t. T_0 (s)	(RA, Dec)	z	Best fit	BIC (null)	Δ BIC	$P_{a\gamma}$	$N_{\rm tot}$, (cm^{-2} MeV^{-1} s^{-1})
090323	259459364.630	(-4, 26)	190.75, 17.07	3.57	`pl`	56.27	4.2	$\sim 10^{-3}$	~ 0
100724B	301624928.090	(5, 27)	123.59, 75.86	-	`pl`	58.66	3.8	$\sim 10^{-2}$	$(1.52 \pm 0.19) \times 10^{-1}$
120624B	362269436.930	(-268, -237)	170.91, 8.94	2.2	`pl`	69.24	3.8	$\sim 3 \times 10^{-2}$	$(1.2 \pm 0.7) \times 10^{-4}$
130504C	389402940.520	(14, 22)	91.55, 3.78	-	`pl`	41.06	3.9	$\sim 10^{-1}$	$(0.9^{+1.8}_{-0.9}) \times 10^{-1}$
160625B	488587220.275	(184, 191)	308.57, 6.93	1.406	`pl`	74.32	4.6	$\sim 10^{-4}$	~ 0
170214A	508779271.920,	(6, 24)	256.32, -1.88	2.53	`pl`	70.12	16.1	$\sim 10^{-2}$	~ 0
221009A	687014224.990	(-1, 5)	288.26, 19.78	0.1505	`Band`	39.76	33.9	$\sim 4 \times 10^{-4}$	$(1.5 \pm 0.4) \times 10^{-1}$

Table 4.2: Out of 93 GRBs detected with LLE, 7 pass the selection criteria imposed in Table 4.1. The time of the LAT trigger is given in the MET format, with the relevant precursor time window denoted relative to the trigger time. The BIC value is given for the null hypothesis (i.e., for a model without an ALP spectral component). The alternative hypothesis includes the ALP component. The difference between BICs is then calculated to determine which model fits the observations better. Between the two models, a better fit is the one with the lower BIC value. Conversion probability values (Fig. 3.4) and the normalization value, $N_{\rm tot}$ deduced from the best fit that has the ALP component. The given value of normalization is in units of 10^{-52} cm^{-2} MeV^{-1} s^{-1}. In bold are shown GRBs observed both with the LLE and the LAT standard data cuts.

GRB Name	T_0 (MET)	Precursor w.r.t. T_0 (s)	RA, Dec	z	Best fit	BIC (null)	Δ BIC	$P_{a\gamma}$	$N_{\rm tot}$, (cm^{-2} MeV^{-1} s^{-1})
090323	259459364.630	(-1, 53)	190.75, 17.07	3.57	`Band`	33.87	1.8 `Band+alp`	$\sim 10^{-3}$	~ 0
090328	259925808.510	(-1, 38)	90.67 -41.95	0.74	`pl`	98.6	1.1 `Band+alp`	$\sim 10^{-2}$	$(5.5 \pm 2.2) \times 10^{-3}$
090720B	269802178.900	(-5, 5)	203.638, -51.198	-	unconstrained	N/A	N/A	$\sim 3 \times 10^{-2}$	N/A N/A
090902B	273582310.320	(-1, 48)	264.95, 27.33	1.82	`Band`	3974.0	733 `Band + alp`	$\sim 8 \times 10^{-3}$	$7.0 \pm 0.4) \times 10^{-4}$
100724B	301624928.090	(-1, 50)	123.59, 75.86	N/A	`pl`	135.11	43.6	$\sim 2 \times 10^{-3}$	~ 0
120624B	362269436.930	(-275, 240)	170.91, 8.94	2.2	unconstrained	N/A	N/A	$\sim 9 \times 10^{-4}$	N/A
130821A	398794231.010	(-900, -840)	314.23, -11.52	N/A	unconstrained	N/A	N/A	$\sim 8 \times 10^{-6}$	N/A

Table 4.3: Out of 255 GRBs detected with LAT, a total of 7 pass the selection criteria imposed in Table 4.1. The time of LAT trigger is given in the MET format, with the relevant precursor time window denoted relative to the trigger time. The BIC value is given for the null hypothesis (i.e., for a model without an ALP spectral component). The alternative hypothesis includes the ALP component. The difference between BICs is then calculated to determine which model fits the observations better. Between two models, a better fit is the one with the lower BIC value. Conversion probability values (Fig. 3.4) and the normalization value, $N_{\rm tot}$ deduced from the best fit that has the ALP component. The given value of normalization is in units of 10^{-52} cm^{-2} MeV^{-1} s^{-1}. Due to low number of counts, we are unable to constrain a best fit model for three of the GRBs.

PRELIMINARY

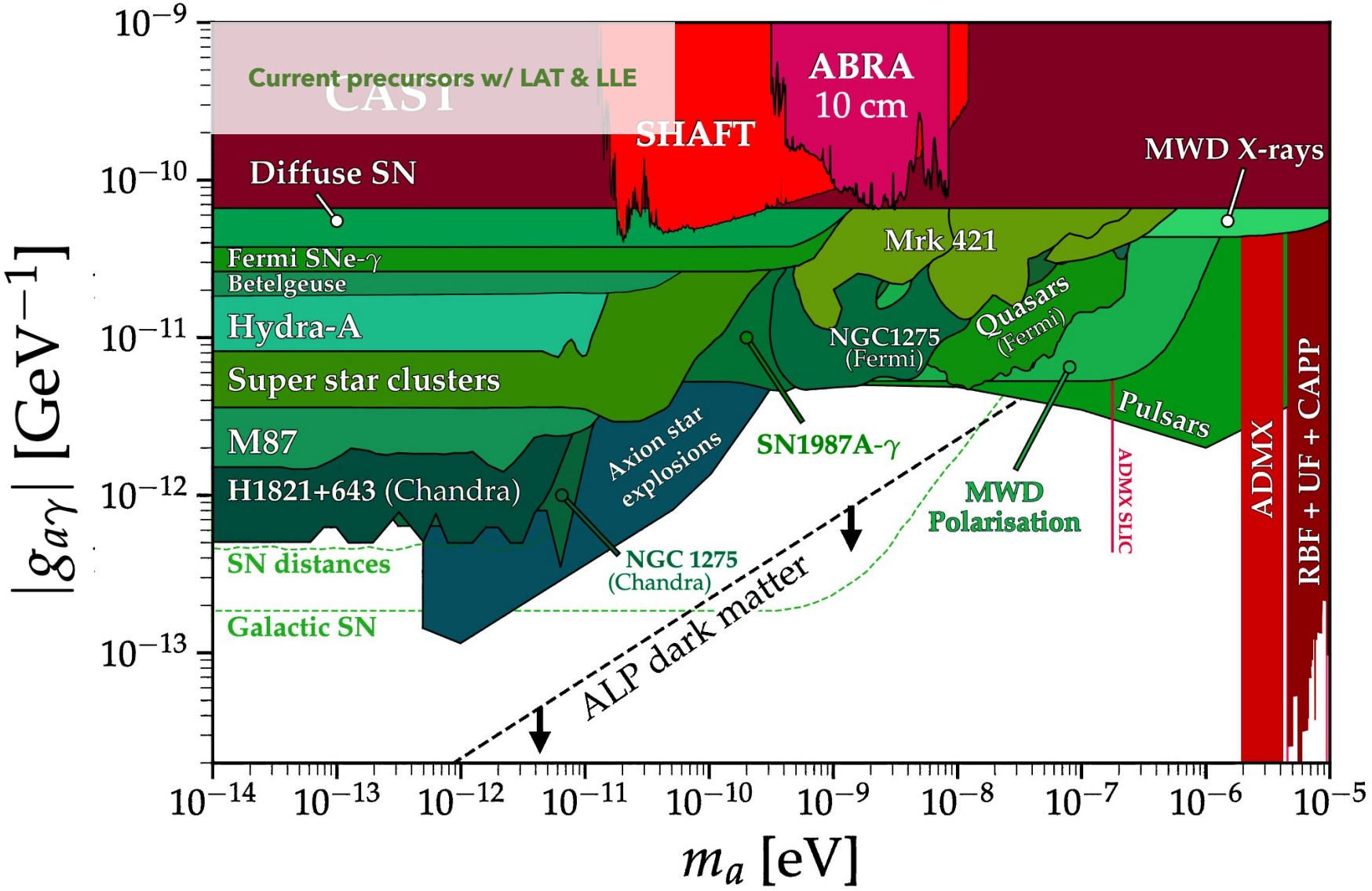

PRELIMINARY

ADDITIONAL CONSIDERATION

Additional considerations: All-sky Medium Energy Gamma-ray Observatory (AMEGO) sensitivity analysis; motivation outlined the Snowmass 2021 Letter of Interest (Prescod-Weinstein et al. 2021, incl. Crnogorčević)

Quick factsheet about AMEGO:

- Probe-class mission concept
- High-sensitivity (200 keV – 10 GeV)
- Wide FoV, good spectral resolution, polarization
- Multimessenger astronomy (NS mergers, SNe, AGN)
- Order-of-magnitude improvement compared to previous MeV missions

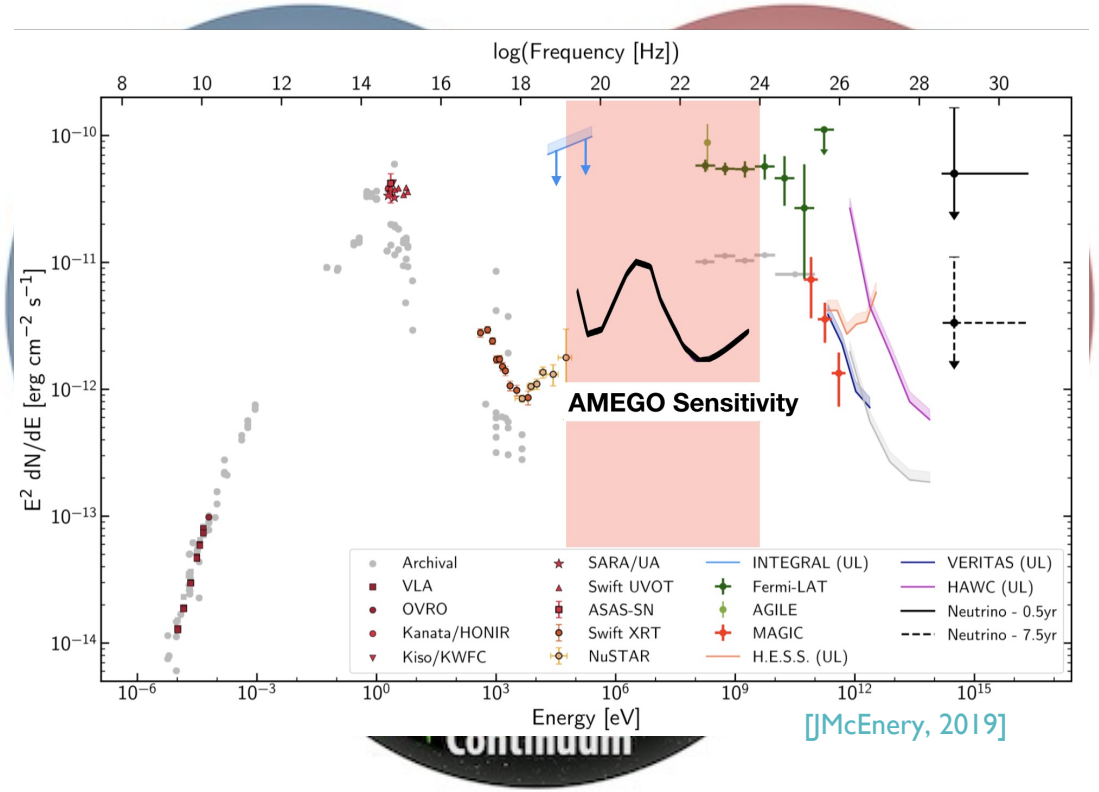

[JMcEnery, 2019]

ADDITIONAL CONSIDERATIO

Additional considerations: All-sky Me sensitivity analysis; motivation outlined the Snowmass 2021 Letter gorčević)

- For a 10-solar mass progenito

levels comparable to LAT in the l

Distance lim

improved by a facto

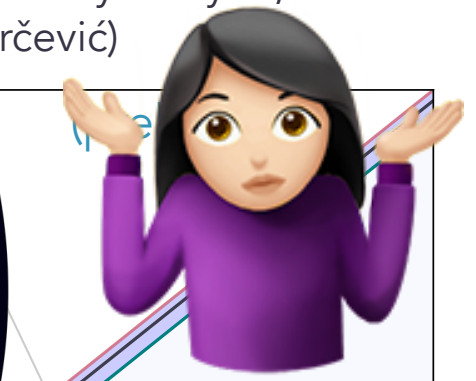

Dark Matter Landscape: An Instrumentationalist's View

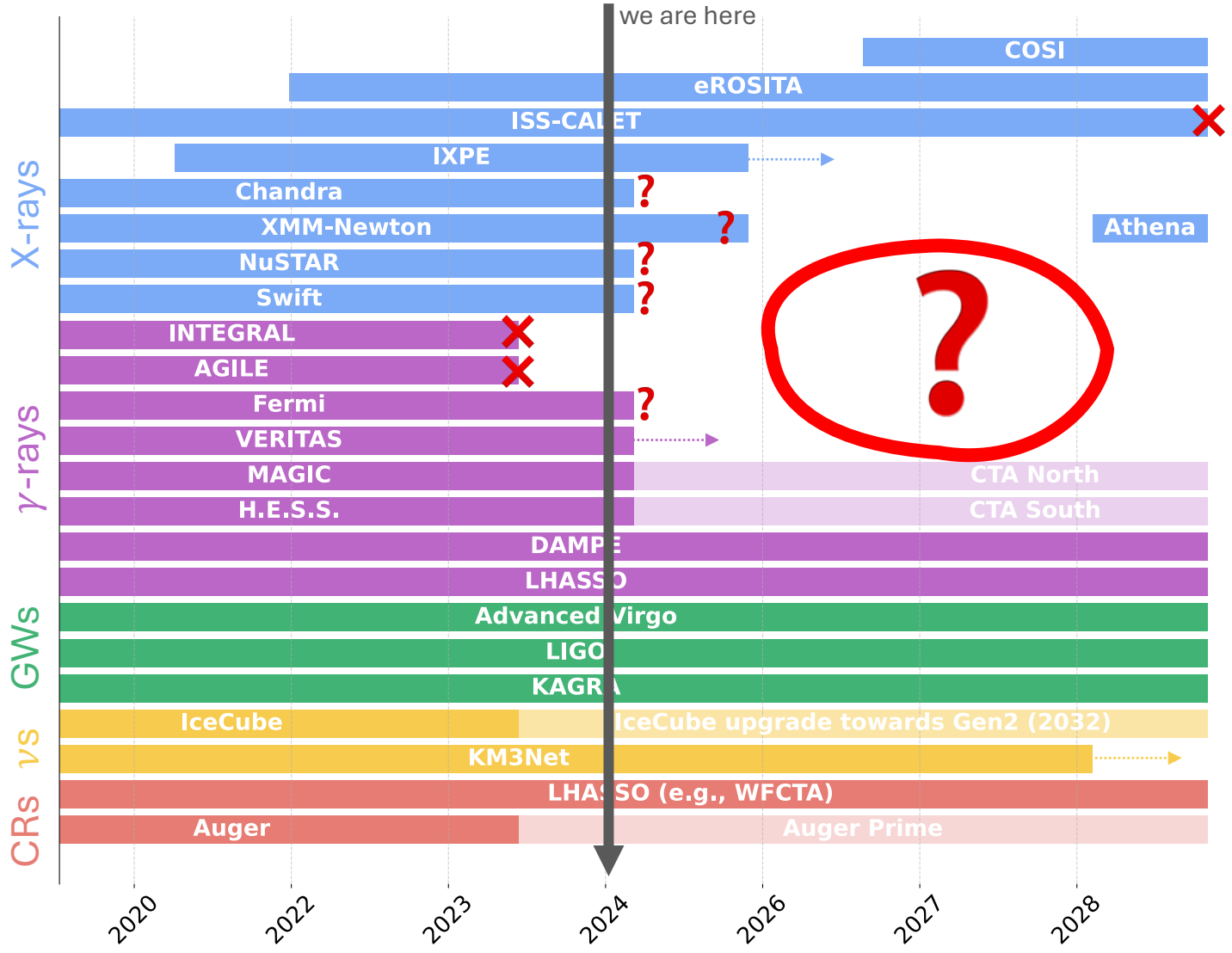

WIMPs

Dark Matter Landscape: An Observer's View

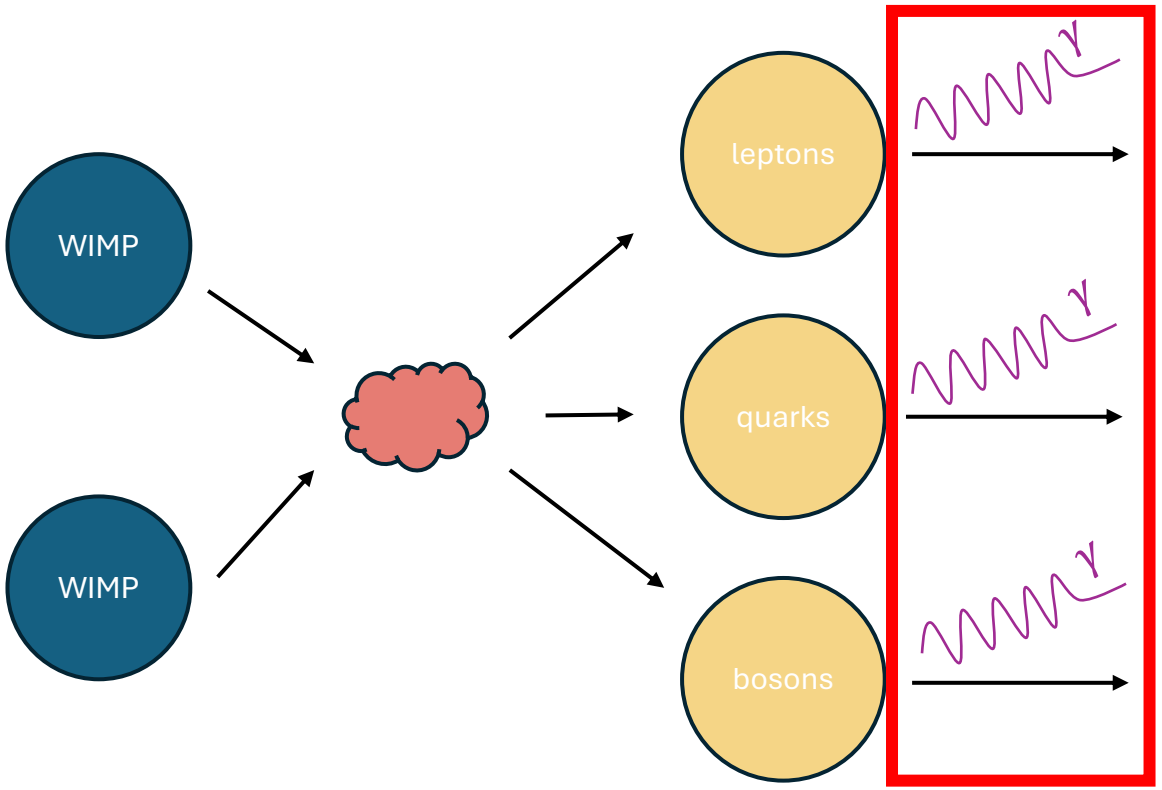

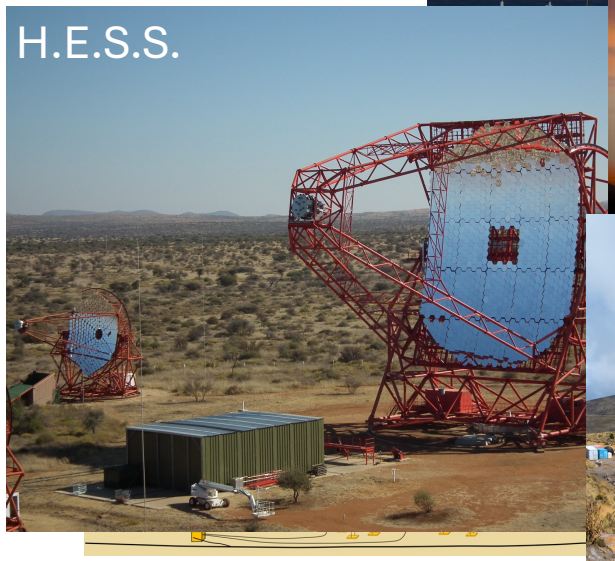

Dark Matter Signal

$$\frac{d\Phi}{dE} \propto \int_{\Delta\Omega,\mathrm{los}} \rho_{DM}^2 \times \frac{\langle\sigma v\rangle}{2M_{DM}^2} \sum B_i \frac{dN_\gamma}{dE}$$

DM γ-ray flux = astrophysics J-factor x particle physics

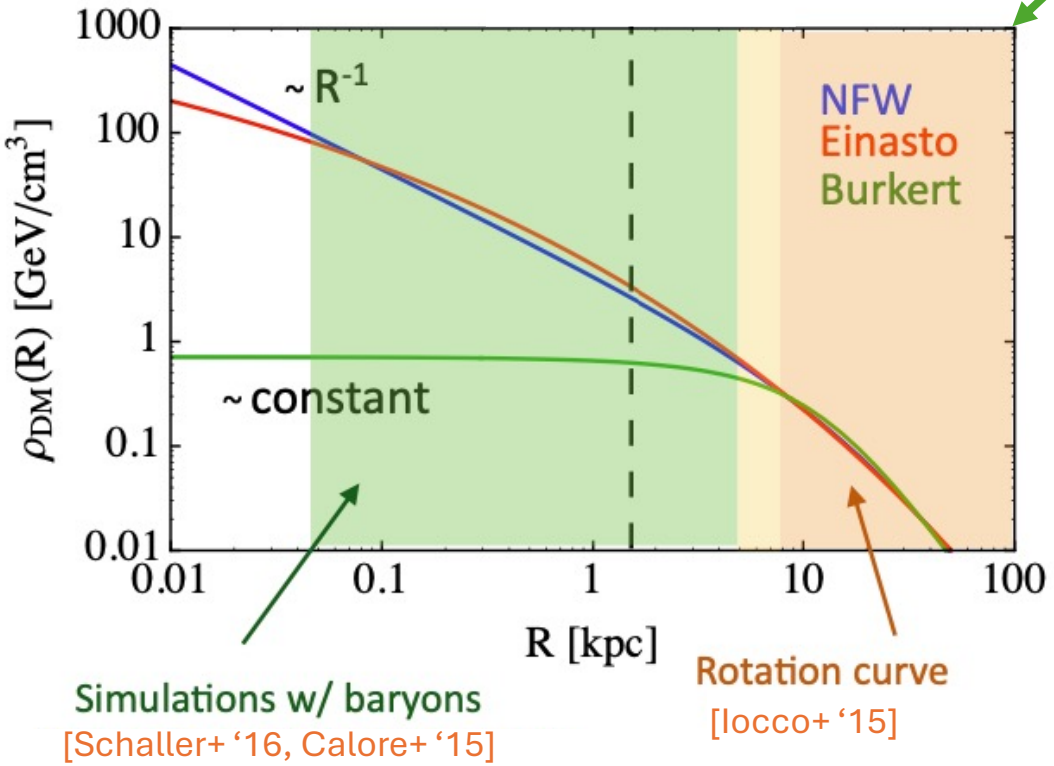

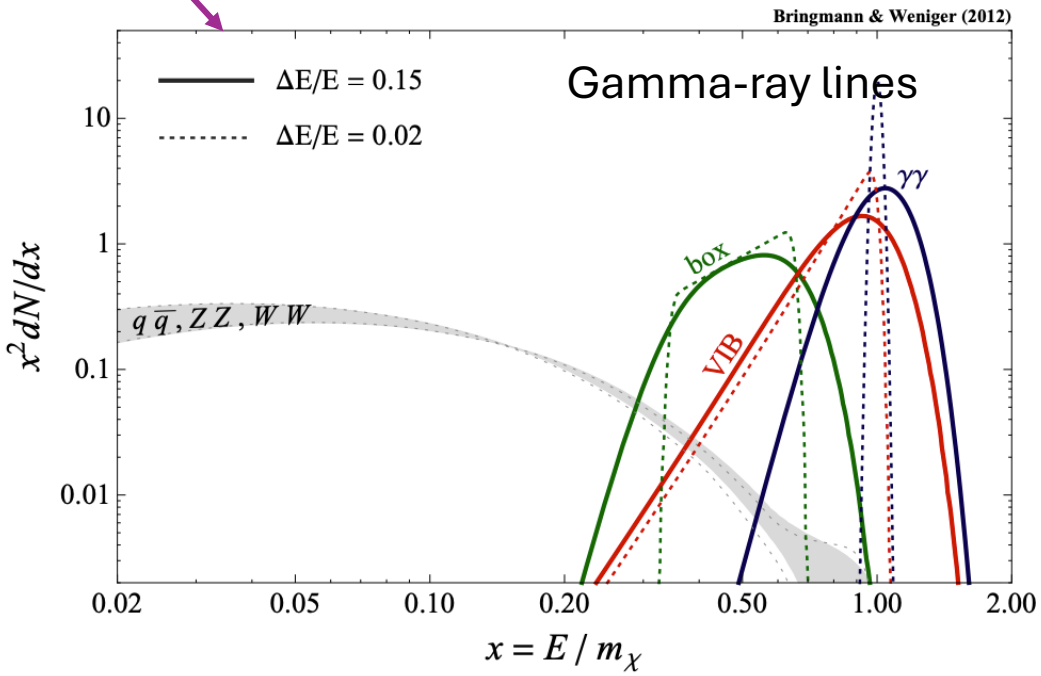

Adapted from F. Calore.

Adapted from Francesca Calore

DM targets

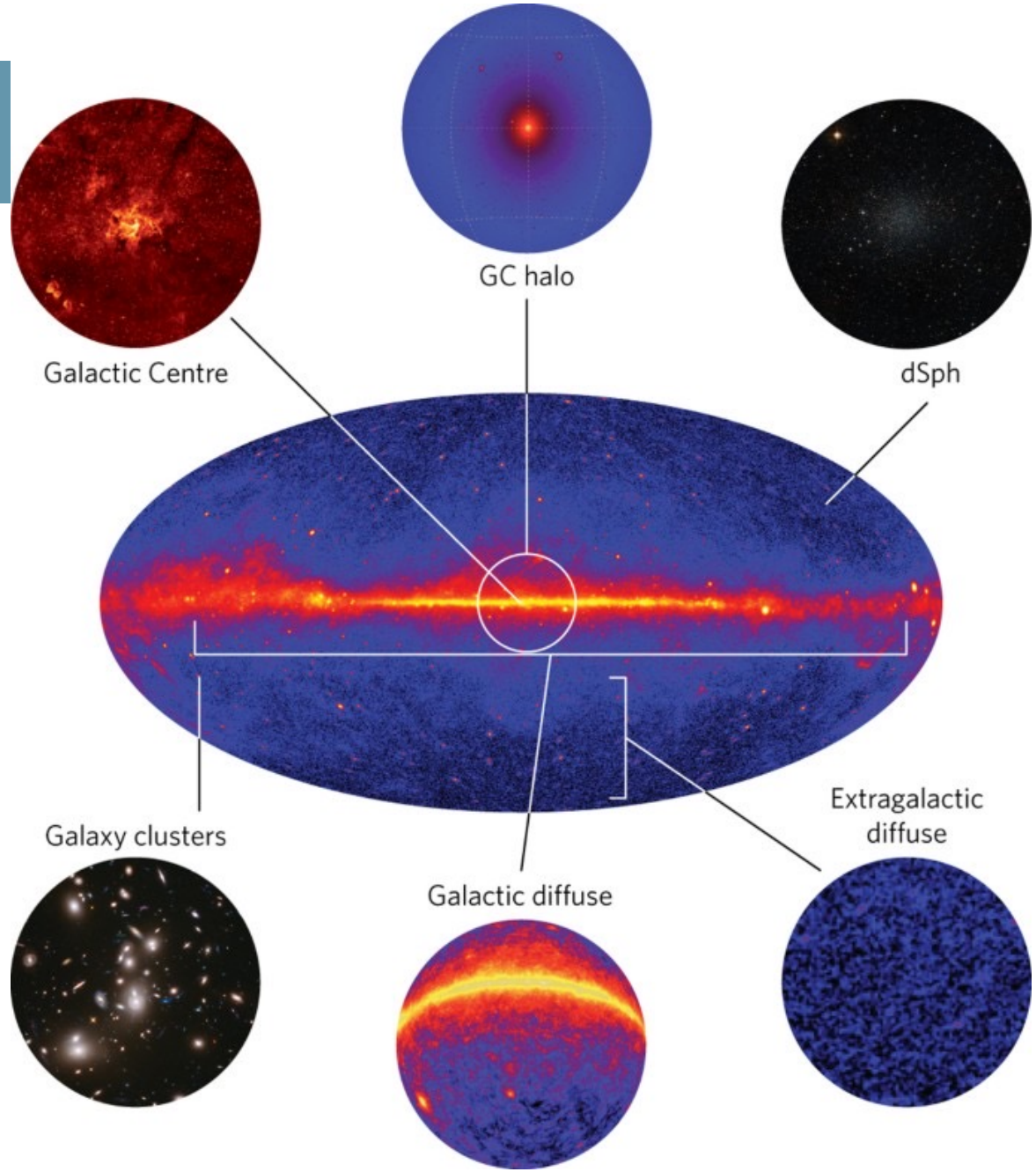

[Conrad & Reimer 2017]

Signal in *Fermi*-LAT

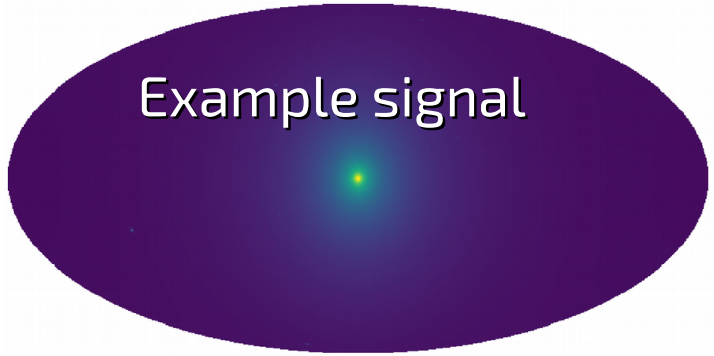

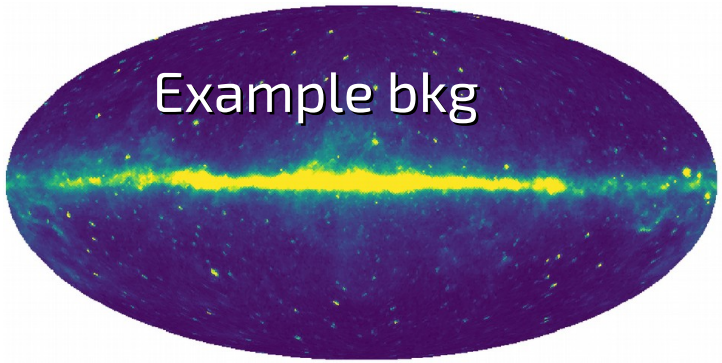

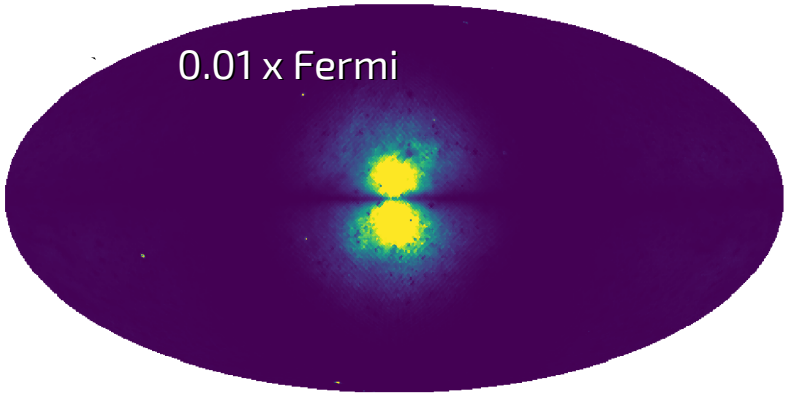

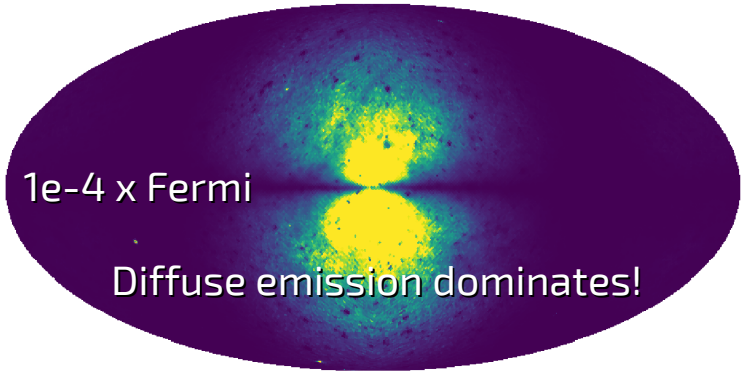

[Adapted from the *Fermi* Summer School]

Dwarf Spheroidal Galaxies

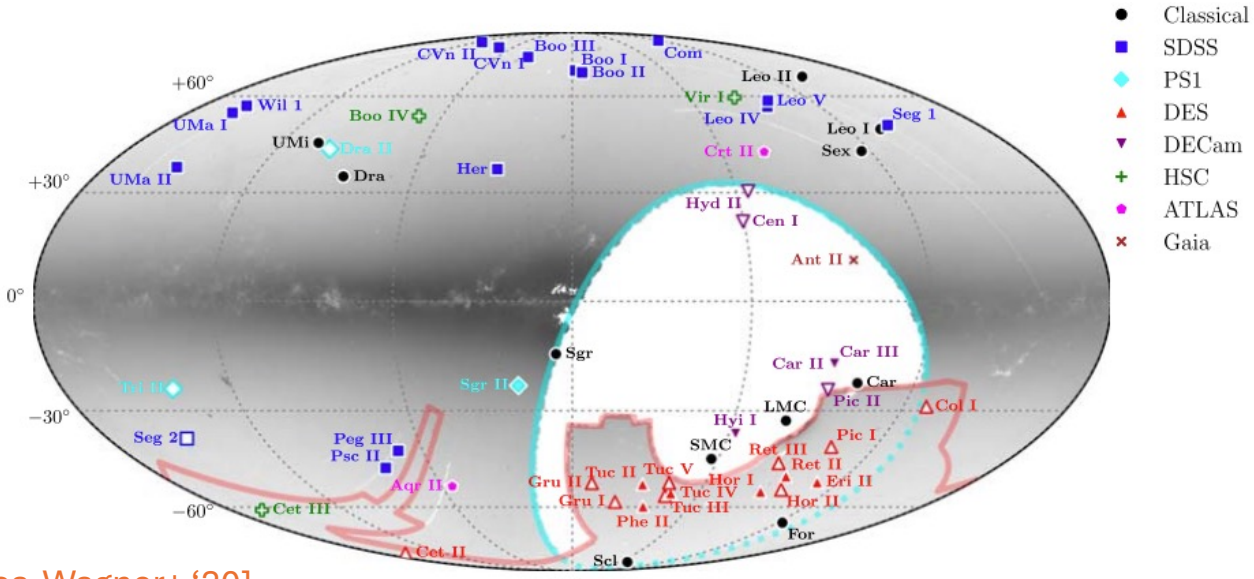

[Drlica-Wagner+ '20]

[McDaniel+ LAT '24]

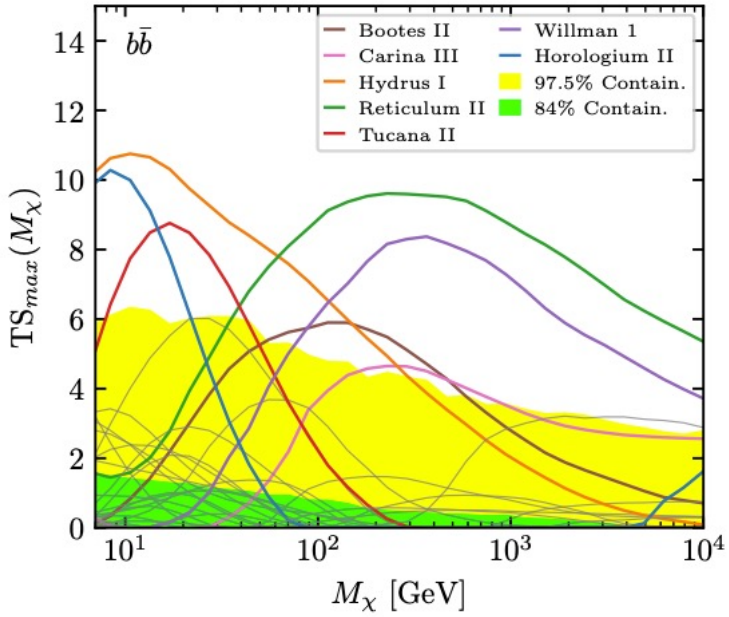

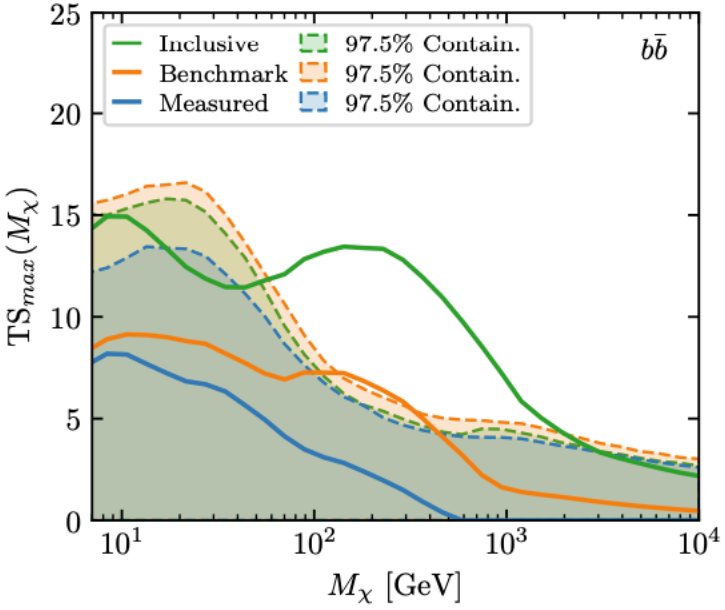

DM γ-ray flux = astrophysics J-factor x particle physics

$$\frac{d\Phi}{dE} \propto \int_{\Delta\Omega,\mathrm{los}} \rho_{DM}^2 \times \frac{\langle\sigma v\rangle}{2M_{DM}^2} \sum B_i \frac{dN_\gamma}{dE}$$

Combined dSph Analyses - Comparison

6 years

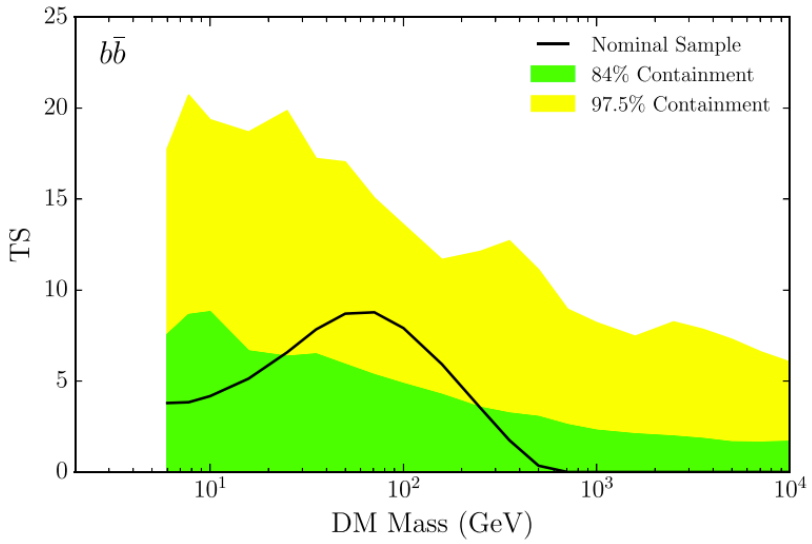

$< 2\,\sigma$

[Albert+ '17]

11 years

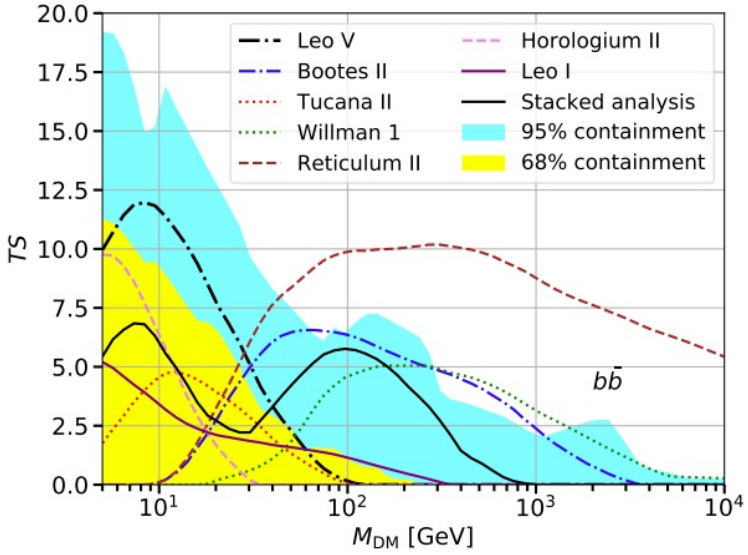

$\lesssim 2\,\sigma$

[DiMauro+ '21]

14 years

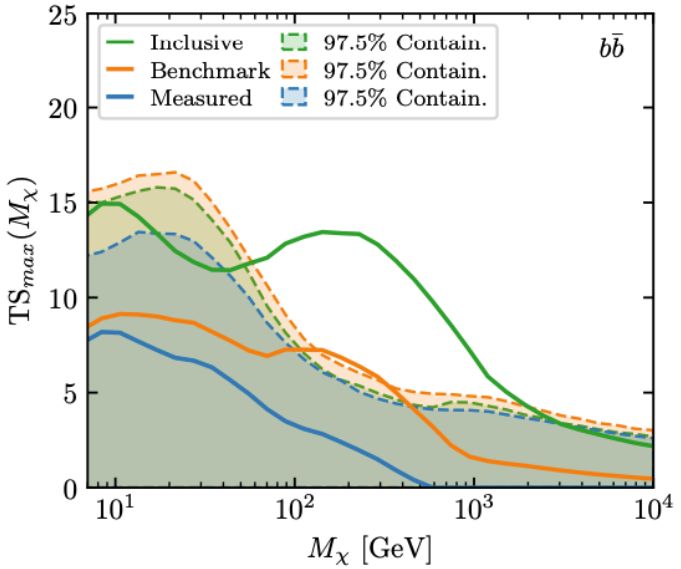

$\gtrsim 2\,\sigma$

[McDaniel+ '24]

Limits on the parameter space

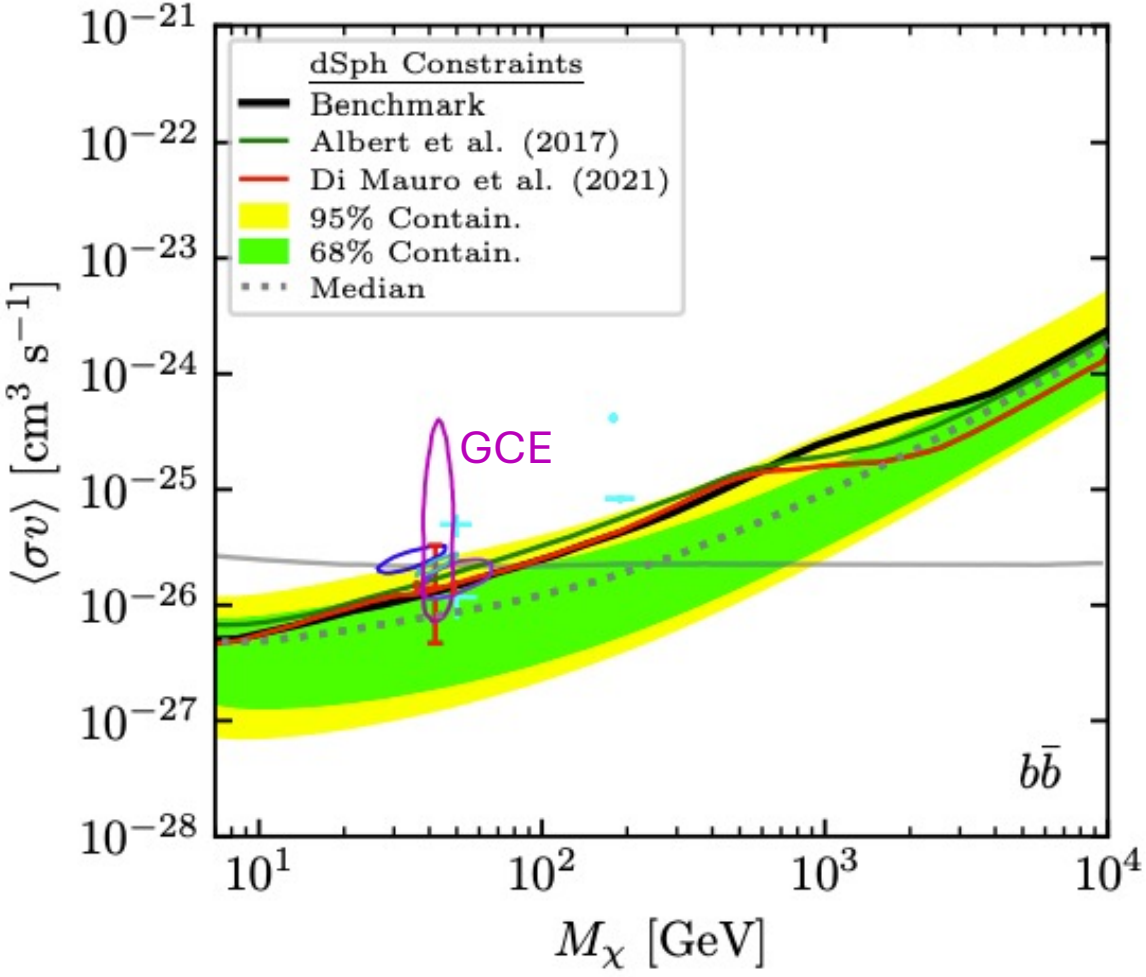

[McDaniel+ '24]

Trials factor reduces significance to 0.5 σ.

- generally consistent with previous limits; *in tension with the GCE results*

- Can we rule DM out? Not yet.

J-values

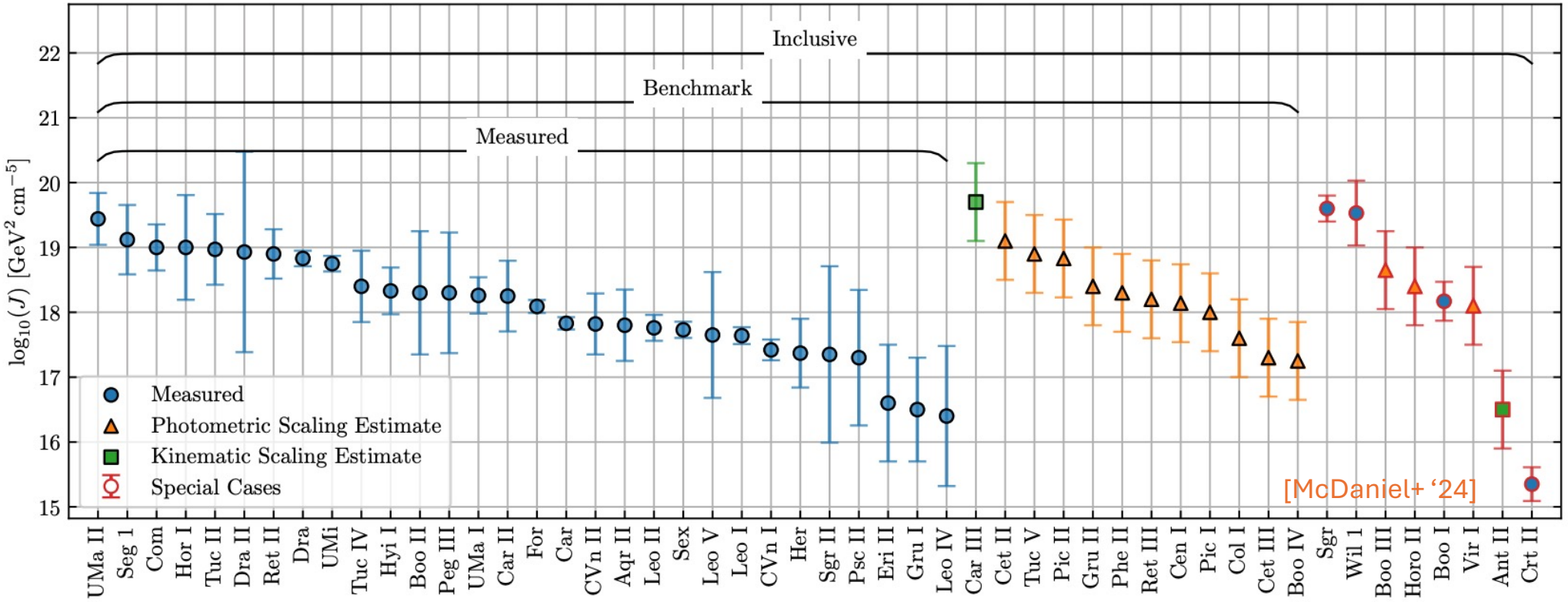

Adapted from a talk from Christoph Weniger.

J-factor considerations:

- Calculations of J-factor values rely on several underlying assumptions (e.g., dark matter distribution models, parametric/non-parametric approaches, observational limitations) [e.g., Bonnivard+ '15, Geringer-Sameth+ '15]
- Triaxiality may affect the J-factor around 2x [e.g., Bonnivard+ '15, Hayashi+ '16]
- Non-parametric approach may reduce the J-factor by a factor of ~ 4 [Ullio & Valli '15]

Future of dSph DM searches

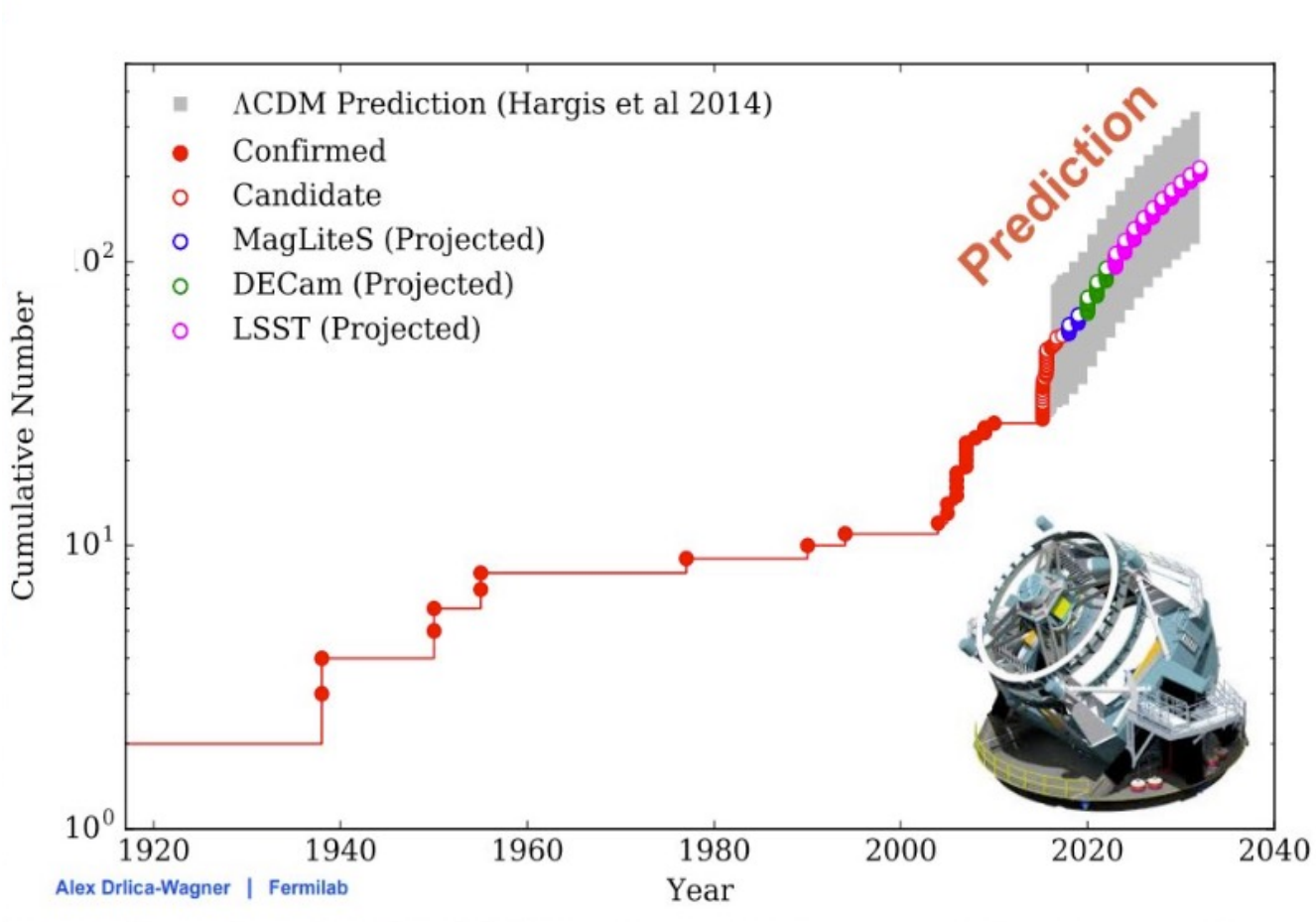

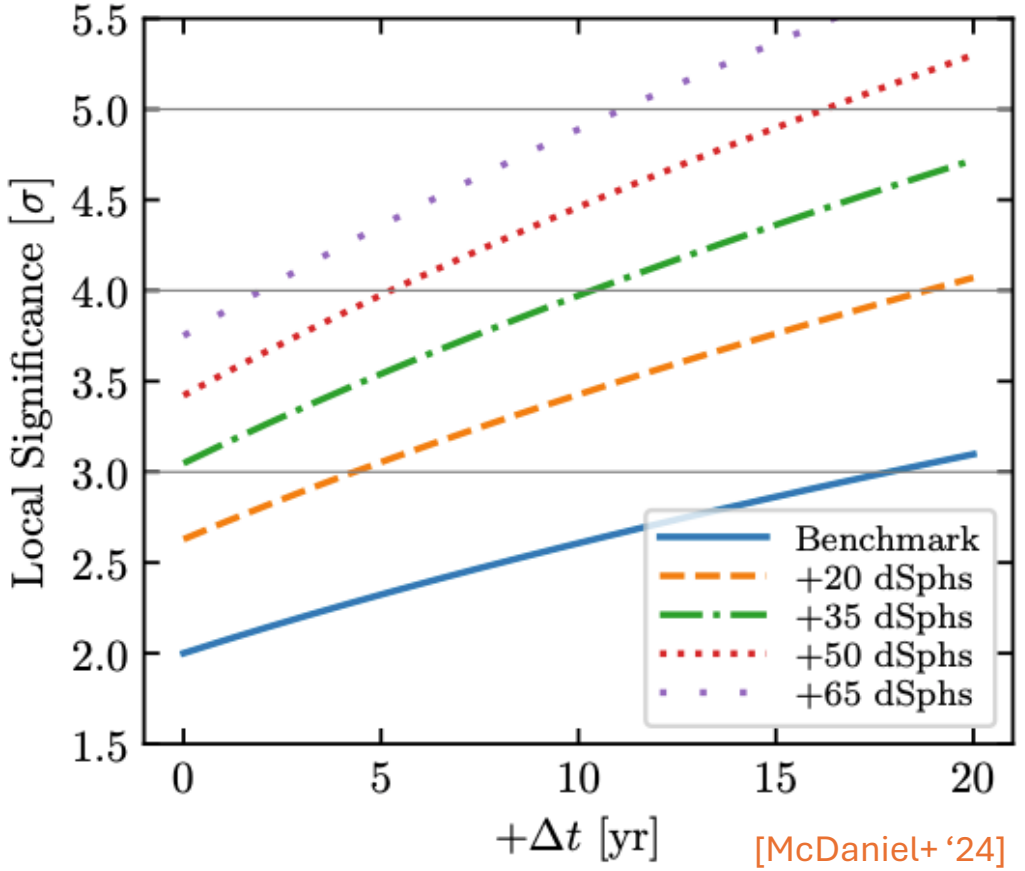

[McDaniel+ '24]

How many dwarf galaxies do we *really* need?

Maybe just one, but a good one?

Ursa Major III

[Discovery: Smith+ 2023]

[J-factor: Errani+ 2023]

- Unstable unless large DM content
- Nearby (~10 kpc)
- Strong constraints on DM annihilation
- *Confirming the dark matter density…*

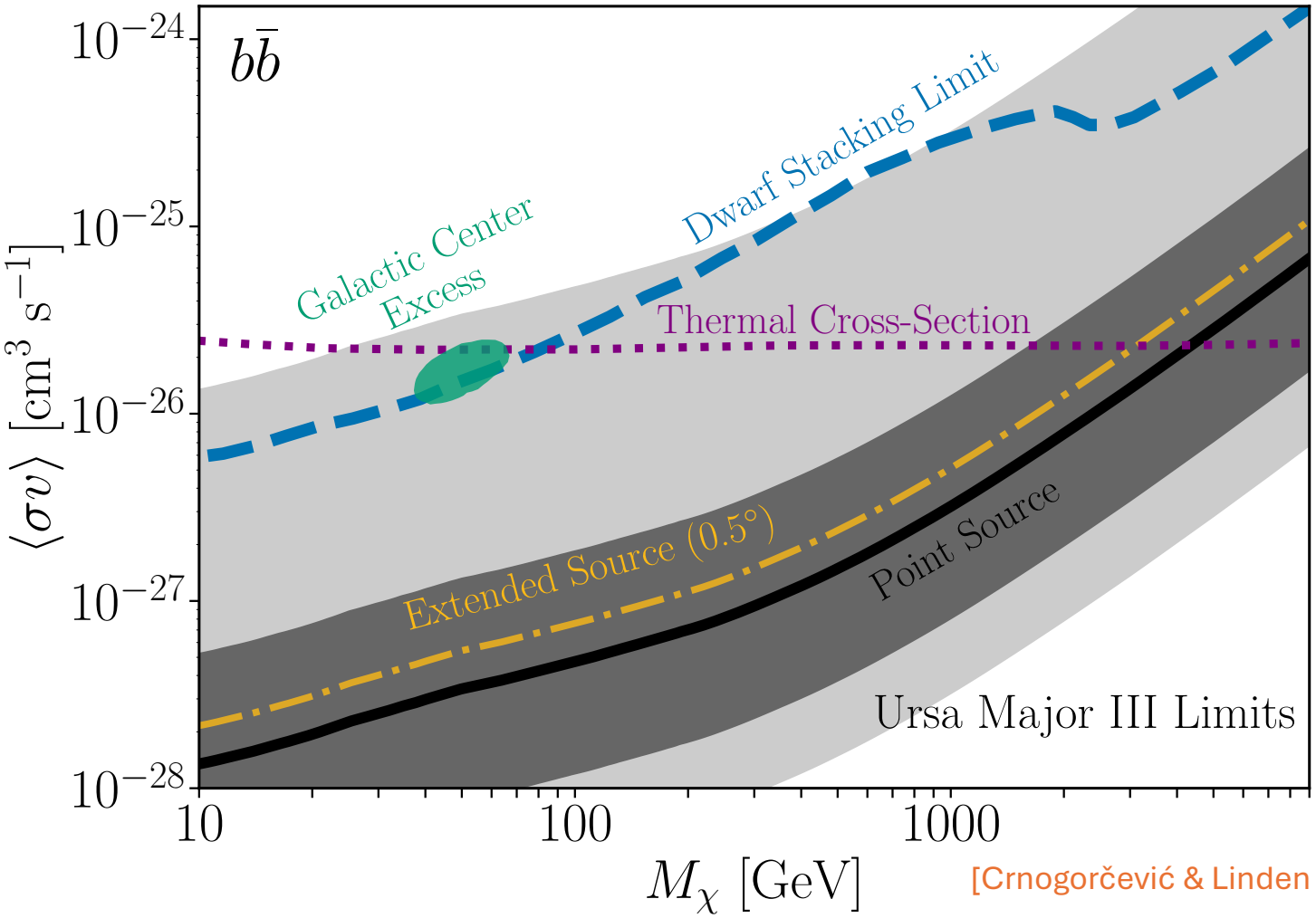

[Crnogorčević & Linden '23]

GloryDuck (LAT, HAWC, HESS, MAGIC, VERITAS)

- Perform multi-instrument and multi-target analysis to obtain the most sensitive and robust results
- Focus: dSphs
- Limits driven by LAT sensitivity
- Legacy analysis of the current-generation gamma-ray instruments

+ LHAASO

Energy coverage

HAWC
300 water Cherenkov detectors
300 GeV to 100 TeV

VERITAS
4 imaging air Cherenkov telescopes (IACT)
85 GeV to 30 TeV

H.E.S.S.
5 imaging air Cherenkov telescopes (IACT)
30 GeV to 100 TeV

MAGIC
2 imaging air Cherenkov telescopes (IACT)
30 GeV to 100 TeV

Fermi-LAT
Space telescope
20 MeV to 1 TeV

MeV GeV TeV

Adapted from Celina Armand TeVPA '22 talk.

GloryDuck (LAT, HAWC, HESS, MAGIC, VERITAS)

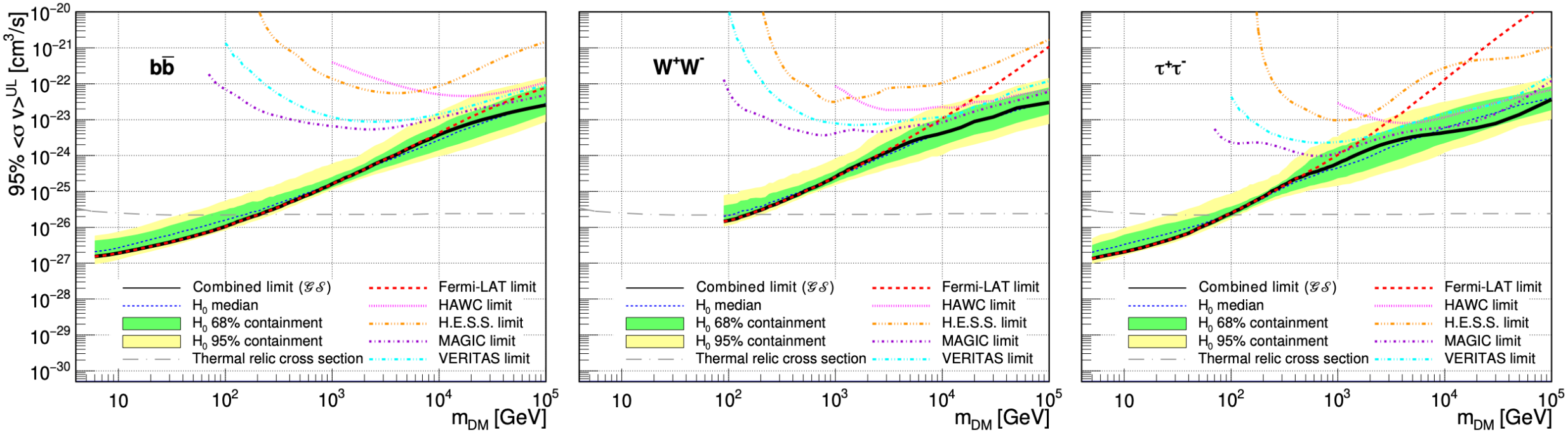

Adapted from Celina Armand TeVPA '22 talk.

GloryDuck (LAT, HAWC, HESS, MAGIC, VERITAS)

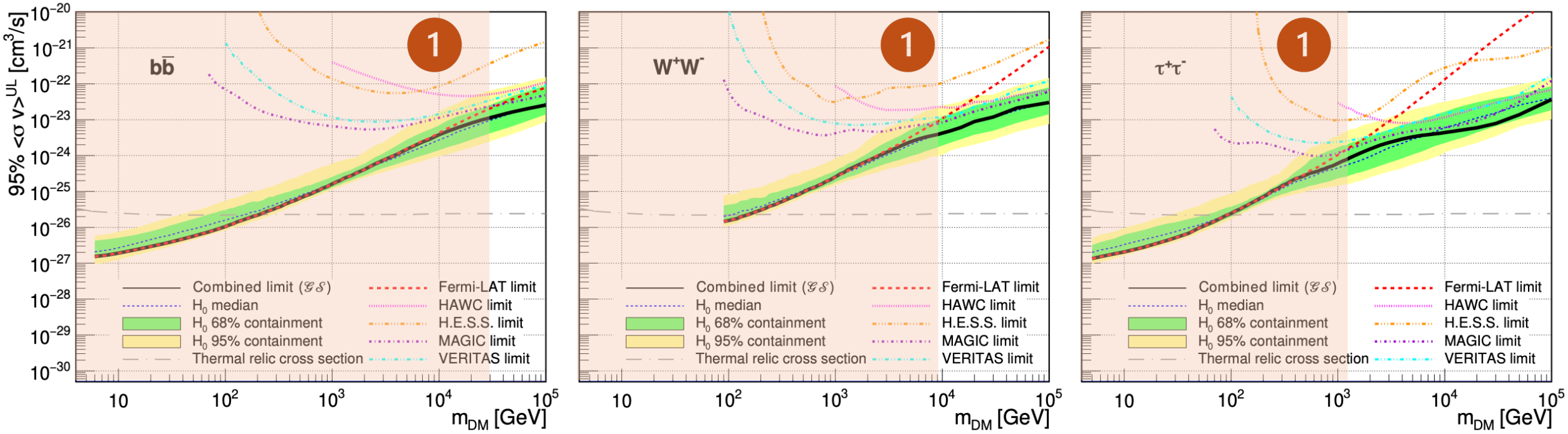

Dominated by *Fermi* LAT 1

Adapted from Celina Armand TeVPA '22 talk.

GloryDuck (LAT, HAWC, HESS, MAGIC, VERITAS)

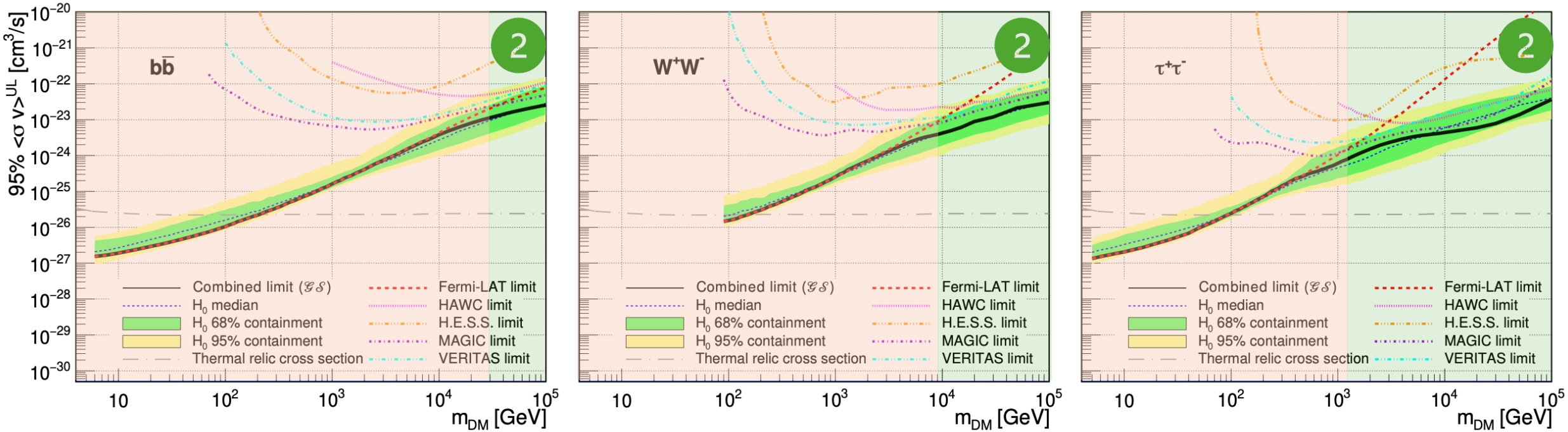

Adapted from Celina Armand TeVPA '22 talk.

HAWC, HESS, MAGIC, VERITAS take over 2

Dark Matter subhaloes, stellar streams, tidal disturbance/stripping of dwarfs, dark matter spikes, brown dwarfs, etc.

Where next?

Dark Matter Landscape: An Instrumentationalist's View

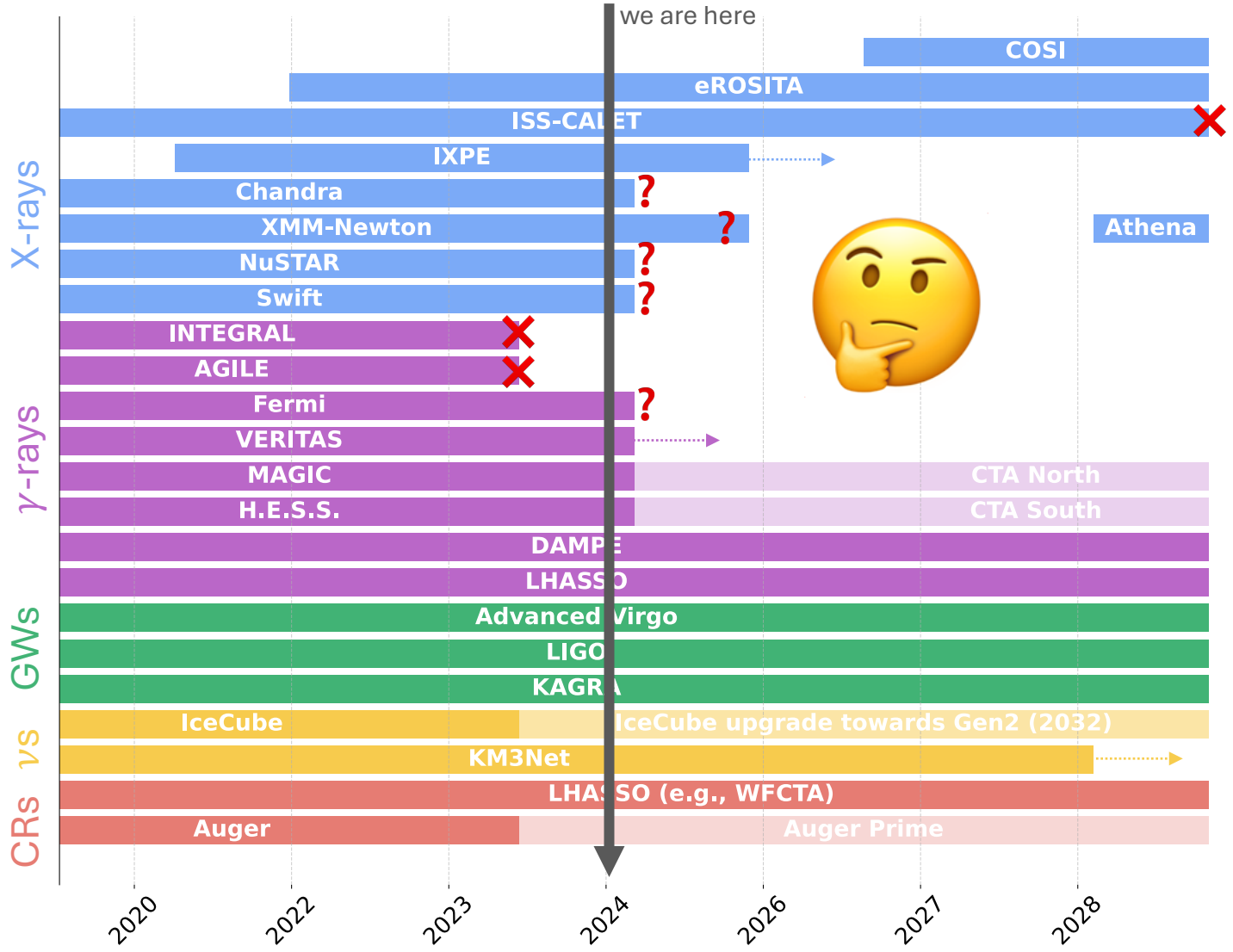

Future Innovations in Gamma rays

Science Analysis Group

… to explore gamma-ray science priorities, necessary capabilities, new technologies, and theory/modeling needs drawing on the 2020 Decadal **to inspire work toward 2040.**

FIG-SAG

FIG SAG Terms of Reference

1. Gamma-ray Science Priorities: Identify opportunities uniquely afforded by gamma-ray observations.
2. Gamma-ray Mission Capabilities: Which science objectives are only done or best done by space-based gamma-ray missions, considering the current missions in extended operation and funded missions in development.
3. Technology Investment: What new technologies/methodologies exist and what is needed to achieve the science priorities.
4. Theory and Analysis Needs: What advances do we need to make in theory and analysis to achieve the science priorities.
5. Synergies with Other Programs: How do these goals tie to the broader astrophysics and physics community. What are the timelines to align with current priorities in multi-messenger astronomy.

Conclusions

- Gamma-ray observations provide unique tests for different dark matter and new physics models
- Indirect detection provides stringent constraints
- Future experiment development is crucial
- Our next space gamma-ray experiment is uncertain---*join FIG SAG to make a strong case to funding agencies: https://pcos.gsfc.nasa.gov/sags/figsag.php*